NASA CR-66861

DESIGN AND APPLICATION OF SELF-COOLED ROCKET NOZZLES

By Peter Schwarzkopf

This publication was prepared by Rocketdyne, A Division of North American Rockwell Corporation, as Report No. R-8057.

Prepared under Contract No. NAS1-7741 by
ROCKETDYNE
A Division of North American Rockwell Corporation
Canoga Park, California

for

NATIONAL AERONAUTICS AND SPACE ADMINISTRATION

FOREWORD

This Final Report was prepared by the Processing Metallurgy Unit, Materials, of the Rocketdyne Research Division, Canoga Park, California, in compliance with G.O. 09047 of Contract NAS1-7741, Part III, Paragraph A.3. The program is administered under the direction of the NASA-Langley Research Center, Hampton, Virginia, with Mr. Richard Mulliken as Project Manager. The report covers the period 5 January 1968 through 31 October 1969.

The heat transfer study was performed by Miss Lydia Manson, Applied Physics Unit, Physical and Engineering Sciences, Rocketdyne Research. Principal Investigator for powder metallurgical nozzle fabrication was D. A. Pearson, Processing Metallurgy Unit.

ABSTRACT

The results of an analytical study to design optimum zinc-infiltrated self-cooled nozzle inserts for a hybrid propellant rocket motor are presented in this report. A computer-programmed heat transfer analysis was used to study the duration of thermal protection of various self-cooled composite designs of different matrix porosities for the anticipated conditions of 6855 F maximum flame temperature and maximum combined film and radiative heat transfer coefficient of 2300 Btu/ft^2-hr-F. A bi-layer composite containing 50 percent porosity in a volume beneath a 20 percent porous throat surface layer was shown to give maximum anticipated service lifetime. A 30 to 40 percent improvement over a tungsten heat sink nozzle was predicted with a self-cooled insert.

CONTENTS

ILLUSTRATIONS

TABLES

INTRODUCTION

Self-cooling thermal protection phenomena offer intriguing technical possibilities in the development of nozzles for advanced solid-propellant and hybrid rocket motors. The throat section of these high-performance motors represents one of the most severe material applications known. Trends toward more energetic, high specific impulse, metallized propellants will exceed the capabilities of available refractory materials. Thermal protection of the nozzle throat is, therefore, a necessity and self-cooling provides a simple, reliable design approach to the optimum utilization of even the most energetic propellants. Furthermore, self-cooled composites can make possible submerged, annular and other advanced nozzle concepts for use with current or future propellant systems.

Self-cooled composite thermal protection is the result of the sacrificial vaporization of a second-phase material from within a porous, structural matrix. Prior analytical and experimental work established those coolant and porous matrix microstructural parameters essential to successful rocket nozzle application of self-cooled composites (Ref. 1,2). A computer program was developed to guide composite design; and, a novel powder metallurgical fabrication process, sequential isostatic compaction, was evolved to translate analytically-derived, graded-porosity matrix designs into actual test hardware (Ref. 2,3). Rocket motor test firings with an advanced propellant confirmed the feasibility of a self-cooled composite concept based on proper combination of coolant with a graded porosity matrix (Ref. 3).

To develop fully the potential of self-cooled composites for rocket nozzle application, additional data are required to demonstrate the quantitative effect of matrix microstructural parameters on service

life expectancy under any given set of firing conditions. Additionally, to develop design confidence in the self-cooled nozzle concept, the consistency with respect to life expectancy of composite inserts of this type must be demonstrated for a given set of firing conditions. The present program was an analytical and experimental effort to design, manufacture, and test inserts to satisfy these design data requirements.

The specific program objectives were twofold: (1) to establish quantitative trade-offs between coolant volume (viz., matrix porosity) and life expectancy of self-cooled inserts of identical envelope dimensions; and, (2) to establish lifetime consistency of self-cooled inserts with all matrix design parameters held constant. The program objectives were to be accomplished by the design and manufacture of two types of inserts containing different matrix porosities.

The designs are based on a computer-programmed analysis of self-cooling used to determine optimum matrix microstructure for a given set of firing conditions. One insert design will be made purposely to have a shorter anticipated service lifetime. Consistency of lifetime performance was to be established by a duplicate firing test of the longer-life nozzle design. One firing test was performed in the hybrid motor facility located at NASA-Langley Research Center. Maximum flame temperature is 6855 F at a chamber pressure of 755 psia with aluminized polyurethane fuel and nitrogen tetroxide (NTO) oxidizer.

STATE-OF-THE-ART SURVEY

SELF-COOLING THERMAL PROTECTION

Early work by several groups of investigators yielded preliminary evidence of a novel intrinsic form of thermal protection possible with a class of composite materials consisting of a refractory porous matrix impregnated with a sacrificially vaporizing second phase. Such materials could operate successfully in hyper-thermal environments which would otherwise melt the dense matrix material. Preliminary evidence of the attractive potential of these composites was demonstrated in applications including high speed wind tunnel throats (Ref. 4), ballistic re-entry body nose tips (Ref. 5,6), and solid-propellant (Ref. 6,7,8) and hybrid rocket nozzles (Ref. 9). The majority of studies focused on tungsten matrix composites containing coolants such as silver, copper (Ref. 4,5,7,8,9), oxides (Ref. 9, 10, 11) inorganic salts (Ref. 7), and organic polymers (Ref. 6).

In order to maximize the thermal protection effects possible with impregnated composites, a basic understanding of cooling mechanisms is necessary prior to application in advanced high-temperature hardware. Several cooling modes were readily apparent: (1) increased effectiveness as a heat sink through greater thermal diffusivity, (2) heat absorption by coolant specific heat, phase changes dissociation, or endothermic reactions, (3) transpiration of vaporized coolant through the depleted porous matrix, (4) reduction of the convective heat transfer coefficient by vapor blocking, and (5) reduction of radiant heat input at the hot gas wall. Although each cooling mechanism is simple by itself, subtle but important complications can be seen to arise since the mechanisms are not independent. For example, efficient transpiration cooling depends upon high mass flowrate: mass flowrate in turn is inversely proportional to coolant latent heat of vaporization; therefore, increased transpiration effects reduce heat absorption capacity.

Other interrelations affecting composite thermal protection performance may exist between matrix and coolant properties. The success of a composite was shown to depend upon parameters of matrix microstructure; i.e., porosity (Ref. 9), permeability (Ref. 12), and powder (or pore) size (Ref. 13). Clearly, optimum coolant-matrix property combinations exist for specific thermal application; and, likewise, an inappropriate combination might explain the observed unsatisfactory performance of certain infiltrated composites in solid-propellant rocket motor nozzles (Ref. 8).

Any attempt at the analysis and subsequent optimization of cooling phenomena must start with the mechanism of coolant movement through the structural matrix. Various investigators have offered different coolant movement theories, resulting in diverse explanations of thermal protection and of methods to maximize cooling effects. Capillary forces have been suggested to motivate coolant flow toward the hot surface to maintain a boiling liquid boundary at a depth beneath the surface dependent upon matrix pore size and heat flux (Ref. 12). If coolant replenishment rate at the boiling interface is too low, the depletion depth becomes too large and surface temperature rises to failure; conversely, too high a flowrate wastes coolant, leading to premature failure. Therefore, optimization of structure for a given application should be possible. Extension of this concept led to the development of two-porosity structures in which the composite had a dense, fine-pored surface (Ref. 12). High density facings presumably have increased capillary pressure, thermal conductivity (to reduce surface temperature) and erosion resistance. Critical values for overlay and bulk composite permeability might exist.

If capillary forces were not of sufficient magnitude to force molten coolant to (or just beneath) the heated surface against the ambient hot gas pressure, consideration must be given to other coolant transfer mechanisms. Thermo-osmosis has been suggested, based on limited

experimental evidence (Ref. 12,14). An encapsulated insert design, to vent coolant vapor in a low-pressure downstream throat region, was proposed to take advantage of this coolant transfer mechanism (Ref. 14). Differential thermal expansion of liquified coolant and the matrix may be another possibility, particularly for high boiling point coolants. A distillation boiler reaction was described for silver/tungsten composites in which differential thermal expansion was presumed to force silver coolant to the heated surface at a rate dependent upon incident heat flux, ambient pressure, and a valving action of the pores (Ref. 15). However, thermal expansion alone was unlikely to account for the volume of coolant lost in nozzle firings (Ref. 15); however, a dependence of composite thermal protection performance on matrix pore size may also be presumed from this mechanism.

Vaporization of coolant from a liquid/vapor interface receding away from the heated surface was the mechanism proposed for low-boiling coolants in more recent work (Ref. 2). Such a mechanism would be analogous to a composite cooled by a subliming material (Ref. 16,17), and it would account for complete coolant losses. An extensive computer-programmed heat transfer analysis confirmed criticality of matrix microstructural parameters such as porosity and permeability on cooling effectiveness (Ref. 1). Application of graded porosity structures was proposed and developed for a category of materials termed "self-cooled" composites (Ref. 2,3). Such composites consist of a denser, low-permeability layer on the nozzle insert throat surface backed by a high-porosity section that acts as a coolant reservoir.

The anticipated duration of self-cooling is greatly extended with increased total matrix porosity. Similarly, surface temperature rise also increases with porosity, an effect related to the inferior thermal conductivity of a highly porous, coolant-depleted matrix. An optimum matrix porosity requires a trade-off between surface temperature and

required lifetime. For example, the rate of coolant recession is slower for a high-porosity matrix. Thus, a steeper temperature gradient can be supported which may lead to premature surface melting. Conversely, a less-porous, more-conductive matrix may be prematurely depleted under identical conditions before surface melting occurred. For single-firing nozzles, a practical design criterion can be as follows: the optimum composite for a given application is that in which coolant is exhausted in the time the surface reaches the matrix melting point (or other temperature limit). Such tailor-made optimum composites would be smaller and lighter, for example, than the counterpart dense tungsten heat sinks which are commonly encountered in solid propellant rocket nozzle design.

Another feature of self-cooling is shown is that as long as coolant is present, the backface temperature cannot exceed the coolant vaporization temperature. Thus, self-cooled composites, like analogous organic ablatives, act as insulators. For comparison, a dense tungsten slab would be practically at uniform temperature when the surface reaches the melting point. A practical result of this secondary thermal protection is that, in addition to cooling the exposed surface, self-cooled composites mitigate the requirement for refractory back-up structures in nozzle assemblies.

The permeability of the exposed nozzle throat layer also critically affects thermal protection performance of self-cooled composites. For self-cooling to work, the coolant must have a boiling (or sublimation) temperature well below the matrix melting point. The coolant must, therefore, boil under the total pressure of both the nozzle throat exhaust gas and the coolant vapor pressure drop through the depleted porous matrix. Thus, if the matrix in the throat were relatively impermeable, as is the case for fine-grained microstructures, coolant boiling could be completely suppressed by the matrix pressure drop.

As a result, the temperature of the vapor/liquid interface would rise unchecked to the hot-gas recovery temperature, and all capability for self-cooling would be lost. Conversely, a more permeable (highly porous or coarse grained) matrix would minimize coolant vapor pressure drop, and the maximum vapor/liquid interface temperature would be fixed thermodynamically at the coolant boiling point.

An optimum maximum permeability has also been shown to exist (Ref. 3). If matrix permeability is too great, coolant may be lost prematurely in the form of large drops. In addition, highly permeable matrices are more subject to exhaust gas penetration in the nozzle convergent section, which can lead to coolant expulsion and pore clogging by oxides of metallized propellants. Therefore, matrix permeability must be tailored for a given set of nozzle operating conditions to allow coolant boiling at a level just sufficient to retard safely throat surface tempature rise during firing. Axial gradations in nozzle throat permeability have been used to achieve an optimum structure (Ref. 3, 14).

Potential coolants include a variety of elements, inorganic or organic compounds, and polymers. Coolants must provide a trade-off between thermophysical properties such as latent heat and temperature of vaporization for optimum duration and magnitude of temperature reduction. In addition, coolants must be chemically compatible with the matrix and environment, and dissociation products must not have a detrimental effect on vehicle performance. This may take the form of reduction of specific impulse, reactivity with other vehicle components, or detection, such as through radar signature. Finally, coolants must be amenable to incorporation into carefully controlled matrix structures during fabrication.

COMPOSITE FABRICATION

That complex, graded porosity structures are required to optimize self-cooling thermal-protection effects is now generally accepted for advanced rocket nozzle designs (Ref. 3,12,14,18,19). Fabrication of composites with the requisite microstructural elements was the essential preliminary to experimental demonstration of the potential of self-cooling. The development of a fabrication process to produce microstructurally complex composites may be resolved into the following steps:

1. Production of different types of uniform porous microstructures with closely controlled properties.
2. Combination of these various microstructures into a structurally integral unit of graded properties.
3. Incorporation of second phase (coolant) within the porous matrix.

Different approaches have been taken utilizing powder metallurgy and have met with varying degrees of success. Plasma-sprayed high-density encapsulation of uniformly porous matrices was the simplest approach (Ref. 14). Test firing of a nozzle of this type of construction did not shown any marked improvement over a similar, unencapsulated composite insert (Ref. 20). Hot-pressing and subsequent bonding together of separate nozzle elements has also been attempted (Ref. 18,19). However, lack of adequate microstructural control and inter-element bonding produced failures in firing tests of experimental nozzles (Ref. 19).

A sequential cold isostatic compaction process to generate complex, graded porosity self-cooled nozzle structures did produce porous matrix microstructures of wide values of porosity and permeability, and it

combined such microstructures into units containing both radial and axial structural variation (Ref. 3). Nozzle inserts produced by the sequential isostatic compaction process were successfully fired in a motor with a propellant flame temperature of approximately 7000 F (Ref. 3).

The problem of accurate geometric location of various nozzle elements of diverse porous microstructure was readily solved by sequential isostatic compaction with the use of shaped molds, mandrels, and machining of green compacts. The technique is illustrated schematically in Fig. 1. However, powder compositions used to form each element varied with respect to molding, pressing, and sintering characteristics. These differences had to be minimized to ensure finished structural integrity of the graded porosity insert and to preclude failures in service by microstructural distortion, shrinkage, or cracking. The flexibility of the powder metallurgical approach based on cold isostatic compaction made possible successful nozzle insert fabrication.

Incorporation of second phase into the uniformly porous or graded matrix completes composite fabrication. The introduction of coolants into a completed, fully sintered matrix is usually preferred for self-cooled composites. In this way, the complex properties of the matrix microstructure, such as the permeability, pore size, porosity, or degree of interparticle bonding, may be predetermined and cannot be altered as might be the case for a co-processing technique in which matrix and coolant powders are mixed prior to consolidation.

Introduction of coolant into a porous matrix may be accomplished in several ways. By infiltration, the finished matrix is brought into contact with molten coolant under vacuum or protective atmosphere. If the molten coolant wets the matrix, it will be drawn into the pores by the action of capillary forces. If capillary forces are insufficient to fill the void volume completely, variations of the infiltration

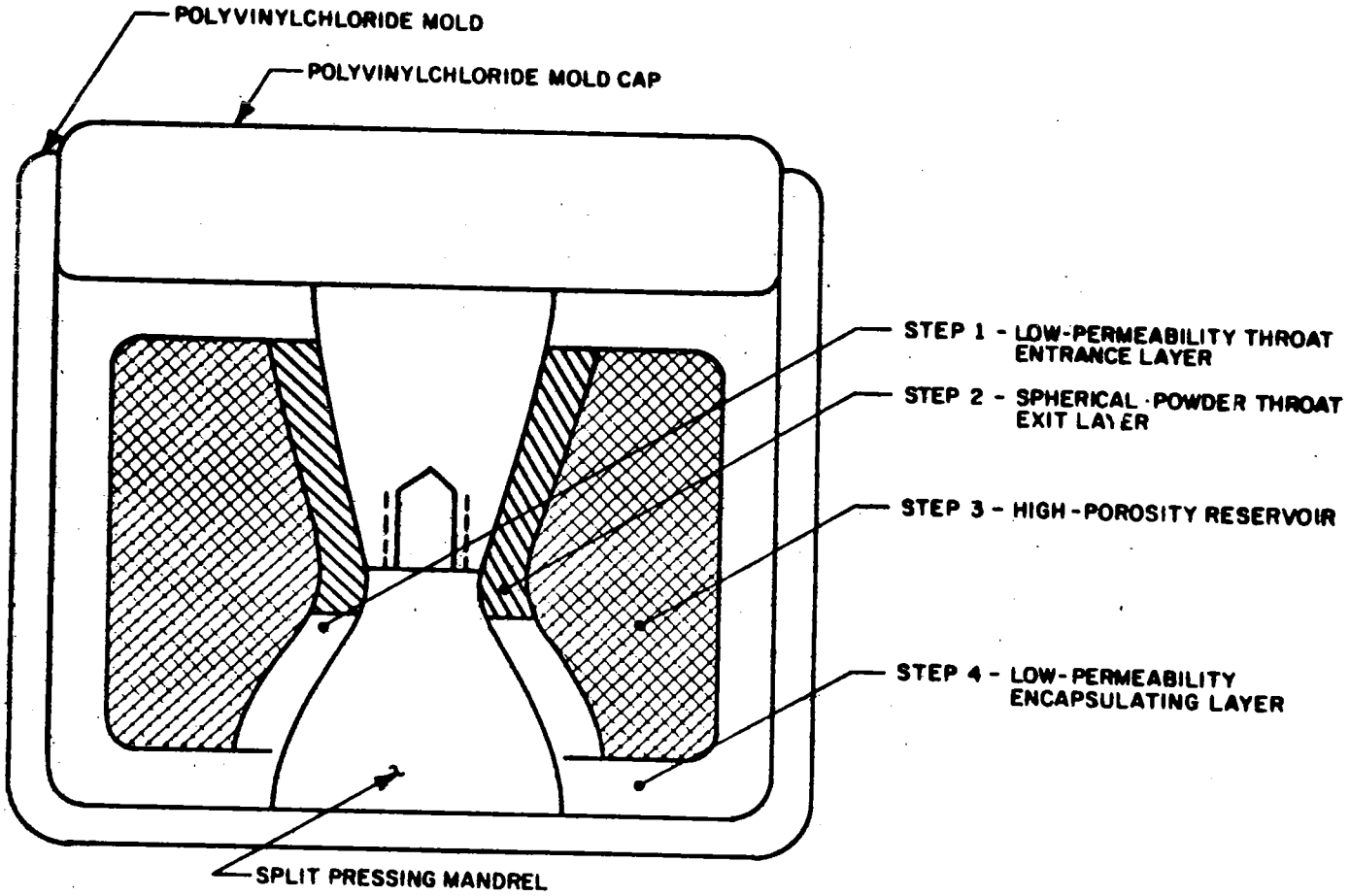

Figure 1. Schematic Diagram Showing the Typical Microstructural Elements of a Graded Matrix Insert Design and the Sequence of Compactions Used in Fabrication.

method may be used. For example, addition of detergents to the unconsolidated powder, to the finished matrix, or to the coolant can be used to promote wetting of the matrix.

Infiltration usually is not difficult on a small scale. As the size of the matrix increases, however, the probability of incomplete penetration also rises. Poor wetting, large pore size, differential thermal expansion of coolant and matrix, coolant solidification shrinkage, and the pressure of undisplaced gases present in the matrix all can prevent complete filling of the matrix pore volume. The use of pressure or vacuum-pressure impregnation cycles, complete immersion of the matrix, degassing additions to the coolant, or directional infiltration and solidification can overcome the problems associated with larger or more porous matrices.

SELF-COOLED NOZZLE DESIGN ANALYSIS

SELF-COOLED NOZZLE COMPUTER PROGRAM

Heat Transfer Model

In a previous study, a comprehensive analytical model for self-cooling was developed to interpret nozzle firing results and, as a nozzle design aid, determine optimum matrix/coolant properties and combinations (Ref. 1). The initial model specified a flat infinite slab of finite thickness, insulated on the backside, and convectively heated on the exposed surface. Coolant was assumed to vaporize from an interface receding uniformly into the porous matrix away from the heated surface. Because of the strong coupling of the partial differential equations describing the continuity, momentum, and energy relations of the model, a closed-form analytical solution was not possible. Consequently, a numerical finite-difference solution was programmed for the IBM 7094 digital computer. Output from the program consisted of transient temperature distributions across the slab thickness, instantaneous coolant vapor flowrate, coolant vapor pressure drop across the depleted, porous matrix, and reduction of the convective surface heat transfer coefficient by coolant transpiration.

The computer program was used to analyze the thermal response of a wide variety of composites based on uniformly porous matrices filled with different types of coolants. The results of case studies for a thermal environment typical of the throat of a high-performance solid-propellant rocket delineated important porous matrix and coolant properties. Specifically, exposed surface temperature rise or the degree of self-cooled thermal protection was primarily dependent on coolant vaporization temperature (at the interface within the matrix), coolant volumetric latent heat of vaporization, and the porosity, thermal conductivity, and permeability of the porous matrix.

An important variable in composite design is matrix porosity which can be controlled within wide limits. In addition to controlling the total amount of coolant available, matrix porosity also governs the location of the cooling interface. Because coolant recession rate is dependent upon volumetric latent heat of vaporization (Ref. 1), the greater the volume of matrix porosity, the slower the coolant recession rate. Therefore, a high value of matrix porosity would tend to maintain a relatively low-temperature coolant interface in the vicinity of the heated surface and so retard temperature rise. However, this effect would be nullified if the resultant matrix conductivity, which decreases with increasing volume porosity, were too low to permit adequate heat flux to the coolant so that surface temperature would rise. Conversely a low-porosity matrix would have a proportionately greater bulk thermal conductivity, but coolant would recede too rapidly from the heated surface, and ultimately would become prematurely exhausted.

Preliminary Design Optimization Study

Two courses are possible in achieving an optimum matrix porosity: (1) a uniformly porous, homogeneous matrix that represents the best trade-off between thermal conductivity and coolant recession rate (i.e., coolant storage capacity); or (2) graded porosity or layered matrix structures in which a low-porosity (high-conductivity) throat surface is backed by a high-porosity coolant reservoir volume. The second approach seemed especially suited for rocket nozzles, since it offers the opportunity of tailoring thermal response and mechanical properties of a self-cooled insert for specific service requirements. For example, a low porosity, high-conductivity throat surface can be designed for maximum erosion resistance, while the back-up layer may be optimized for coolant storage. The graded porosity concept provided a flexible means to design optimum self-cooled nozzle throat inserts. As a result, the computer program was modified to include variable

matrix porosity and permeability as a function of depth from the heated surface (Ref. 3).

Calculations made with the modified program indicated that significant increases in service lifetimes were possible with graded-matrix-porosity self-cooled inserts (Ref. 3). However, inserts had to be optimized with respect to the anticipated service conditions since the expected failure mechanism was dependent on thermal conditions. For example, under conditions of high heat flux and high gas temperature, insert lifetime would be limited by surface melting before complete coolant exhaustion. Conversely, coolant exhaustion would limit insert lifetime under more moderate heat transfer conditions. The performance improvement of a self-cooled insert over a more conventional heat sink nozzle was also shown to depend on nozzle throat heat transfer conditions. These preliminary design considerations were borne out in rocket motor firing tests (Ref. 3), and they formed the basis for nozzle design in the present program.

COMPUTER PROGRAM MODIFICATIONS

Axisymmetric Conversion

To improve the accuracy of the analysis and computer-based predictions of insert lifetime, the Self-Cooled Nozzle Computer Program (Ref. 1, 2) was modified to accommodate axisymmetric configurations. The original program was based on the solution of a one-dimensional heat conduction equation

$$\rho C \frac{\partial T}{\partial \theta} = \frac{\partial}{\partial x}\left(k \frac{\partial T}{\partial x}\right) \qquad (1)$$

where ρ, C and k, the composite density, heat capacity and thermal conductivity, respectively, can vary with temperature, T, and Θ is the exposure time, and X, the distance from the heated surface.

The program was changed to accommodate cylindrical coordinates. The conduction equation in the axially-symmetric two dimensional case is

$$\rho C \frac{\partial T}{\partial \theta} = \frac{1}{r} \frac{\partial}{\partial r} \left(K r \frac{\partial T}{\partial r} \right) \tag{2}$$

where r is the radius.

The modification was carried out by multiplying the density and the conductivity k by a factor r/r_*, where r_* is the throat radius of the self-cooled throat insert. The above operation is equivalent to a change in coordinates, as follows:

Let $x = r - r_*$; then $\partial x = \partial r$ and equation (1) reads

$$\rho C \left(\frac{r}{r_*} \right) \frac{\partial T}{\partial \theta} = \frac{\partial}{\partial x} \left(K \frac{r}{r_*} \frac{\partial T}{\partial x} \right) = \frac{\partial}{\partial r} \left(K \frac{r}{r_*} \frac{\partial T}{\partial r} \right) \tag{3}$$

or

$$\rho C \frac{\partial T}{\partial \theta} = \frac{1}{r} \frac{\partial}{\partial r} \left(K r \frac{\partial T}{\partial r} \right) \tag{4}$$

which is identical to equation (2). Thus, the introduction of the (r/r_*) factor in density and conductivity values is equivalent to a change to cylindrical coordinates for the conduction of heat.

The heat balance equation yielding the mass flowrate of coolant gas per unit area G_c generated by evaporation of the coolant at the interface $(r = r_v)$ is not affected by the change to cylindrical coordinates, but the coolant mass flowrate G_r at any position r between the interface r and the nozzle surface is increased by a factor of r_v/r. The pressure drop in the coolant gas is a function of the mass flowrate per unit area so that if the appropriate value of $G_r = G_c (r_v/r)$ is used at a given position r in the wall, the correct pressure drop will be obtained without any further modification of the equations.

Radiation Correction

Another modification to the original Self-Cooled Nozzle Computer Program was the addition of a radiative component to the heat transfer coefficient. Since the aluminum loading of the NASA-LRC hybrid solid-propellant is relatively high (45%), radiation from liquid aluminum or aluminum oxides may be significant. Discussion of the magnitude of the radiative component and prediction of nozzle throat conditions are included in the following section.

ESTIMATED NOZZLE THROAT CONDITIONS

Heat flux to the nozzle throat is a function of gas recovery temperature (viz., adiabatic wall temperature) and the convective and radiative coefficients of heat transfer between propellant species and the throat surface. The estimated gas temperature was calculated by means of the Rocketdyne Propellant Performance Computer Program (Ref. 21). Input, based on data furnished by NASA-LRC (Ref. 20), to the program is given in Table 1. Calculated propellant performance data are given in Table 2.

The calculated nozzle gas recovery temperature was 6600 F, a value limited by the usual assumption of uniform mixture ratio distribution and chemical equilibrium. A maximum theoretical flame temperature of 6855 F was given, but, depending on mixture ratio, a value as low as 6740 may be obtained (Ref. 20). To obtain a conservative estimate of throat insert life and gain some insight into the effect of gas temperature on insert surface heating, calculations were made for gas recovery temperatures of 6855 and 6740 F.

The convective heat transfer coefficient, calculated by the simplified Bartz method (Ref. 22), was 1670 Btu/ft^2-hr-F. Accurate estimation of the radiative heat flux was hampered by uncertainties in the evaluation

TABLE 1

INPUT DATA FOR PROPELLANT PERFORMANCE EVALUATION
AND CONVECTIVE HEAT TRANSFER COEFFICIENT CALCULATION

Propellant: fuel - polyurethane
+ 45 percent aluminum

oxidizer - nitrogen tetroxide (NTO)

(no additional binders, inhibitors, etc., included in calculation)

P_c, chamber pressure psia	755
O/F, oxidizer: fuel ratio	1.56
Gg, mass flowrate, lb/in^2-sec	5.10
$(Rc)_d$, Reynolds Number	1.31×10^6
C_{pg}, specific heat, Btu/lb-F	0.421
T_o, initial temperature, F	70
r_*, throat radius, inches	0.625

TABLE 2

CALCULATED NOZZLE THROAT CONDITIONS

T_s, temperature, F	6600
P_*, throat pressure, psia	436
h_c, convective heat transfer coefficient, Btu/ft^2-hr-F	1670
h_r, radiation heat transfer coefficient, Btu/ft^2-hr-F	300-1000

of wall and particle emissivities and particle temperature. The propellant performance analysis confirmed the expectation of the presence of aluminum and aluminum oxides in the propellant exhaust stream. Dependent upon emissivity and particle temperature assumptions, heat transfer coefficients of 300 to 1000 Btu/ft^2-hr-F were calculated for radiation. Therefore, it was decided to study the performance of proposed insert designs for three values of heat transfer coefficient, reflecting various contributions by radiation. The values selected were 1700, 2000 and 2300 Btu/ft^2-hr-F.

THROAT INSERT DESIGN CALCULATIONS

Design Envelope

The geometry of the insert design envelope used for analysis is given in Fig. 2. Basically, the insert consists of a low porosity throat layer backed by a higher porosity coolant reservoir volume. The reservoir layer is backed by a low porosity encapsulating layer which in turn is surrounded by a graphite heat sink, one-half inch thick. Throat diameter used in all calculations was 1.249 inches, and insert outside diameter, 3.750 inches. Porosity in the throat and encapsulating layers were fixed at 20 percent, and encapsulating layer thickness fixed at 0.125 inches. The coolant selected was zinc. Prior experience had shown zinc to combine desirable thermophysical properties (e.g., boiling point, latent heat of vaporization per unit volume) with tungsten matrix chemical compatibility and ease of infiltration (Ref. 3).

Properties of the porous tungsten matrix and zinc coolant are given in Table 3. Matrix permeability constants were used in the following equations to calculate coolant vapor pressure drop across the depleted matrix:

$$\frac{P_v^2 - P_*^2}{\delta} = 2\alpha \frac{RT_r(\mu_c G_c)}{gM} + 2\beta \frac{RT_r (G_c)^2}{gM} \qquad (5)^*$$

*Note that Eq. (5) is an approximation. The one-dimensional flow equation was converted to axisymmetric form to obtain this solution.

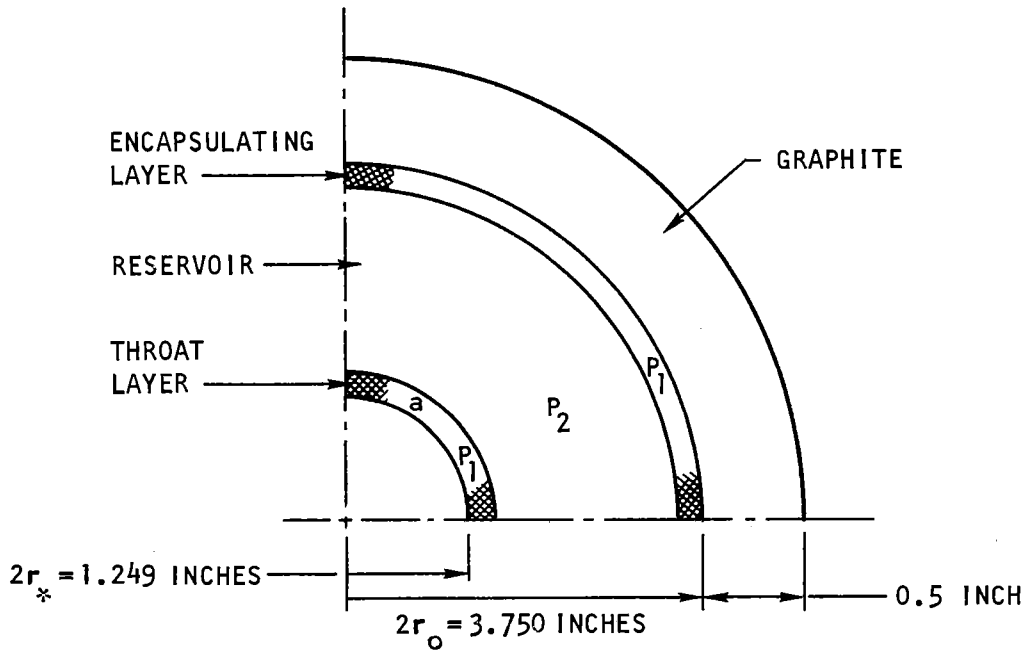

Figure 2. Self-Cooled Nozzle Insert Design Configuration

where α and β are porosity-dependent permeability constants; P_v, the coolant vapor pressure at the receding interface; P_*, the throat stagnation pressure; f, the depth of coolant depletion; R, the universal gas constant; g, the gravitational constant; μ, coolant vapor viscosity; G_c, coolant vapor flowrate; M, coolant vapor molecular weight; and, T_r, the average coolant temperature through the depleted zone. Values of matrix permeability for the various porosities used in the design calculations are given in Table 4.

TABLE 3

MATRIX AND ZINC COOLANT PROPERTIES

	Tungsten	Zinc
M, atomic weight	183.92	65.38
$(Cp)_g$, vapor specific heat, Btu/lb-F	--	0.076
Cp, solid specific heat, Btu/lb-F	0.0385	0.130
, density, lb/ft^3	1204	445.0
k, thermal conductivity, Btu/hr-ft-F	60.0	40.0
T_{vo}, boiling temp. at 14.7 psia, F	--	1663
T_c, critical temperature, F	--	3786
vo, boiling latent heat, Btu/lb	--	810

TABLE 4

TUNGSTEN MATRIX PERMEABILITY CONSTANTS

Matrix Porosity percent	α ft^{-2}	β ft^{-1}
20	10^{10}	10^6
50	10^9	10^5
60	5×10^8	5×10^4
70	2×10^8	2×10^4
80	10^4	10^4

Comparison of One-Dimensional and Axisymmetric Programs

The conversion of the Self-Cooled Nozzle Computer Program from the one-dimensional slab model to axisymmetric form in cylindrical coordinates resulted in somewhat greater predicted lifetimes. This result was expected since the heat sink effect and the availability of coolant would naturally be greater due to annular geometry. The calculated difference was not large, however, for the 1.249 inch throat diameter which constituted an O.D. to I.D. ratio of 3. An example of the calculated difference in surface temperature history for the two models is given in Fig. 3. For the given set of nozzle conditions, insert failure was predicted by tungsten melting according to the one-dimensional model at a time when the zinc coolant was nearly exhausted. The axisymmetric program predicted failure due to zinc depletion with a 3.5 second longer lifetime.

Insert Design Characteristics

The fundamental criterion used for self-cooled insert design analyses was that coolant exhaustion was to occur at the same time as the surface temperature reached the matrix melting point. The principal design variable was matrix porosity (viz., the reservoir porosity) to trade-off matrix thermal conductivity and coolant storage capacity. Fulfillment of this matrix design criterion for a given set of nozzle throat conditions, characterized by gas temperature and heat transfer for coefficient, will be shown to result in longest insert lifetime.

Matrix reservoir porosities and throat surface layer thicknesses for the insert designs analyzed are presented in Table 5. Insert configuration was as depicted in Fig. 2. To bracket the response of various designs as a function of throat environment, calculations were made for two gas temperatures with three values of the heat transfer coefficient at each gas temperature.

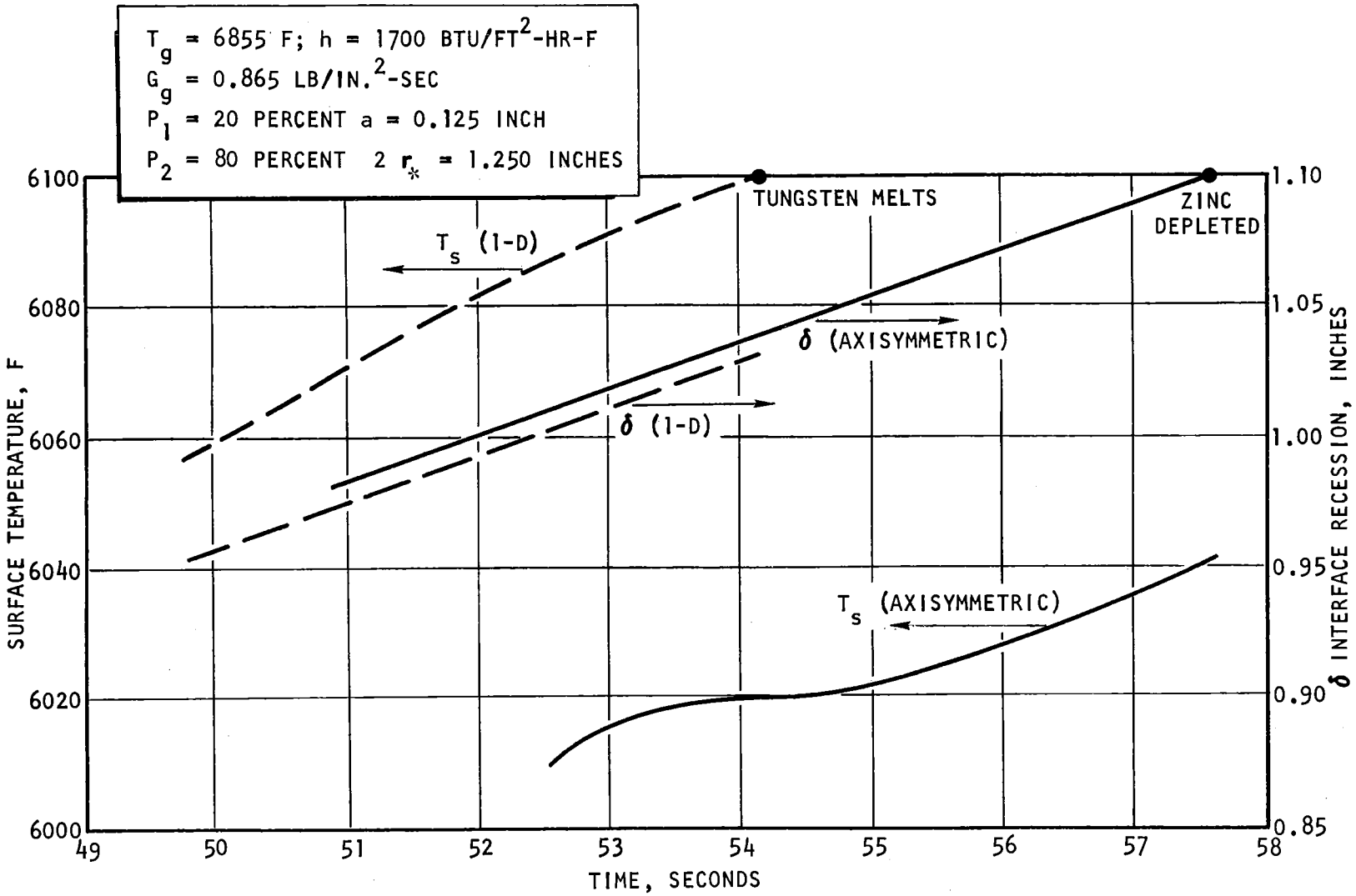

Figure 3. Comparison of Surface Temperature and Interface Recession Depth Values Obtained with the One-Dimensional and with the Axi-Symmetric Computer Programs for Tungsten/Zinc Throat Inserts

TABLE 5

INSERT DESIGN PARAMETERS

Design No.	Surface Layer Thickness, in.	Reservoir Porosity, percent
1	0.125	80
2	0.125	70
3	0.125	60
4	0.125	50
5	0.125	40
6	0.250	60
7	0.375	60

Firing conditions of differing severity make comparison of the merits of any given design difficult. To provide a basis for comparison and obtain a figure of merit, the surface heating of a solid tungsten throat insert under the various firing conditions was calculated as shown in Fig. 4.

The data of Fig. 4 may also be used to compare predicted insert lifetime with the results of actual firings in the NASA-LRC hybrid gas generator (Ref. 20). Failure times for a wrought tungsten and silver/tungsten composite inserts are presented in Table 6. From Fig. 4 wrought tungsten would be expected to start melting after 24.7 seconds under the most severe conditions (h = 2300 Btu/ft^2-hr-F), a value nearly equal to the actual failure time. Somewhat longer failure times were recorded for the silver/tungsten composites which have somewhat higher heat capacity and thermal diffusivity and are, therefore, more efficient heat sinks than dense tungsten. The simplifications inherent in the two dimensional model and physical undertainties in what actually constituted insert failure (taken as chamber pressure drop) would make the agreement of predicted and experimental failure times presented in Table 6 appear fortuitous. Nevertheless, the nozzle throat conditions of the NASA-LRC hybrid may be expected to be on the more severe side of the thermal spectrum considered in the design analysis.

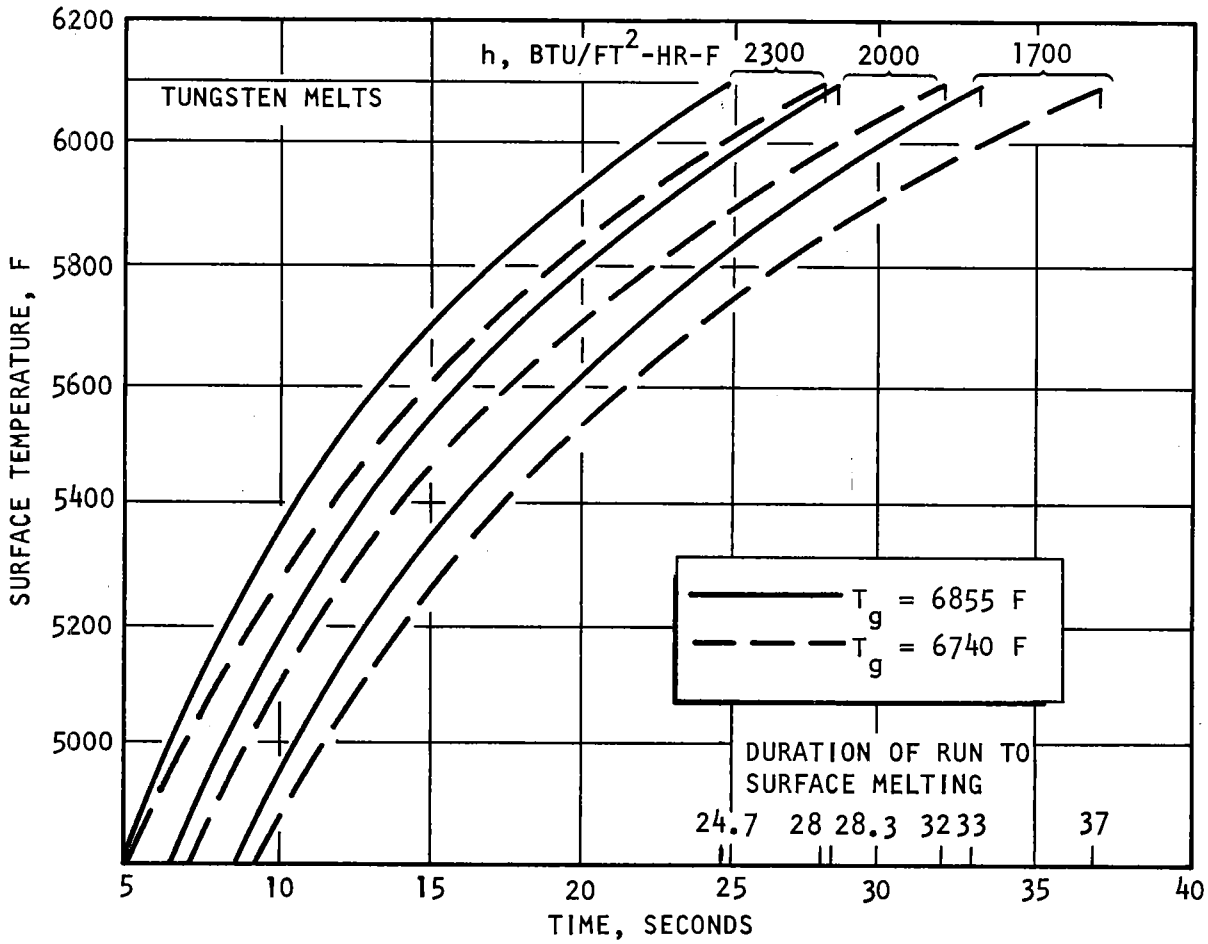

Figure 4. Calculated Surface Temperature of a Dense Tungsten Throat Insert Backed by a 1/2-Inch Graphite Heat Sink Under Various Heat Transfer Conditions

TABLE 6

PREDICTED TIMES FOR TUNGSTEN INSERT SURFACE MELTING AND OBSERVED FAILURE TIMES FOR NASA-LRC EXPERIMENTAL TUNGSTEN AND SILVER/TUNGSTEN INSERTS

Insert Type	Est. Gas Combustion Temperature, F	Observed Failure Time, sec.*	Predicted Failure Time, sec. h = 2300	Predicted Failure Time, sec. h = 2000
Forged W	6835	24.5	24.7	28.3
Ag/W (Polaris type)	6755	33.0	28.0	32.0
Ag/W (Arde-Portland)	6740	31.3	28.0	32.0

Run durations were calculated for insert designs containing 40, 50, 60, 70, and 80 percent reservoir porosity (Designs 1 through 5, Table 5) and the results plotted according to failure mode in Fig. 5. When failure was due to tungsten matrix surface melting (6100 F), the residual depth of zinc coolant was plotted on the upper portion of the ordinate. Conversely, for a failure due to zinc depletion, the value of surface temperature at the time of coolant exhaustion was plotted on the lower portion of the ordinate. According to the design criterion, the failure point plotted in Fig. 5 for a given set of thermal conditions would lie in the vicinity of the melting/depletion boundary for a near-optimum value of matrix porosity.

Comparison of run duration of self-cooled with dense tungsten inserts under identical nozzle throat conditions is presented in Fig. 6. Run duration ratio, plotted as the ordinate, is the time to failure of self-cooled insert divided by the time to surface melting of an identical dense tungsten insert (Fig. 4).

The data presented in Fig. 5 and 6 show the importance of optimizing insert porosity for the particular nozzle throat conditions expected in practice. In general as gas temperature and heat transfer coefficient

*To 20-percent drop in chamber pressure

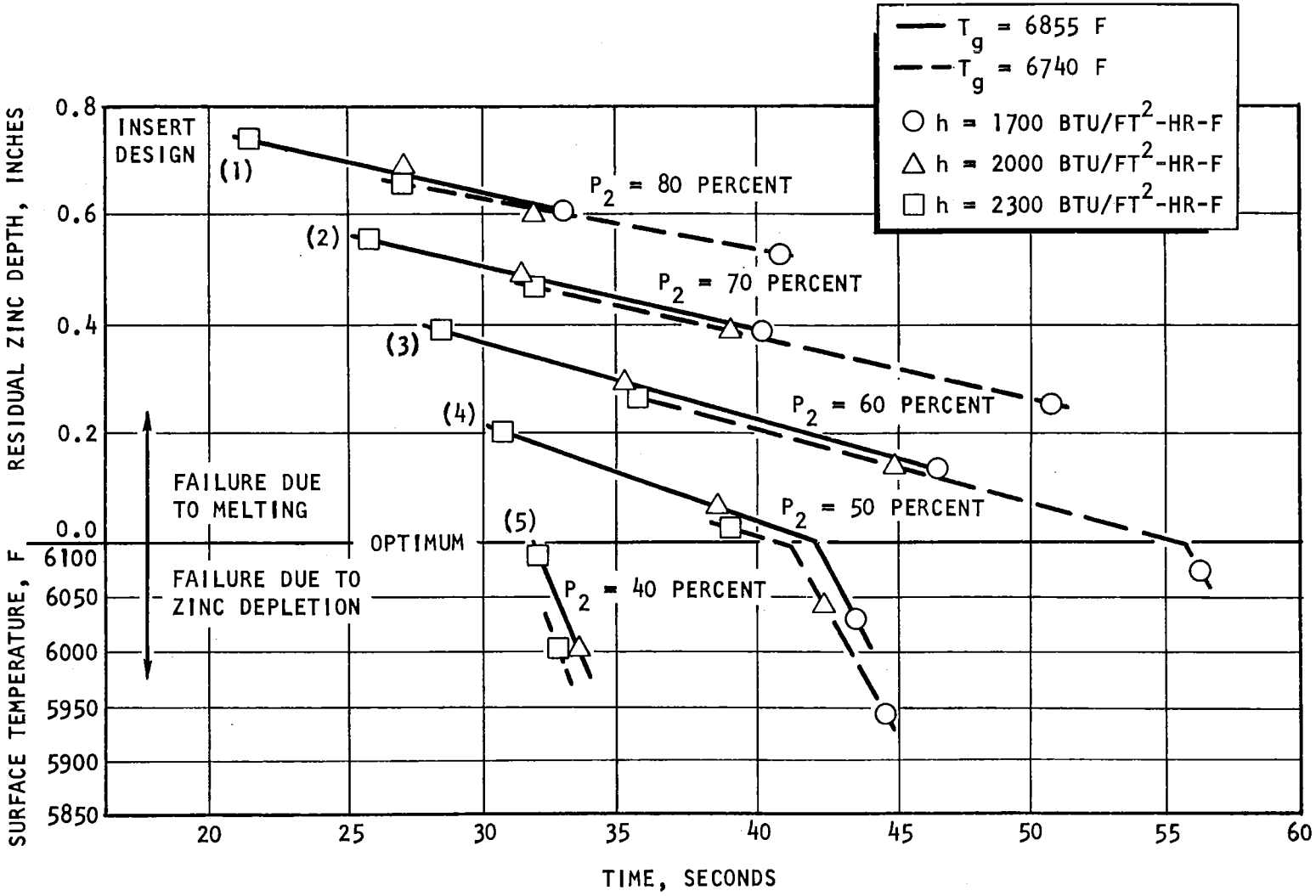

Figure 5. Run Duration to Failure for Tungsten/Zinc Throat Inserts with a 1/8-Inch-Thick Low-Porosity Layer (Predicted)

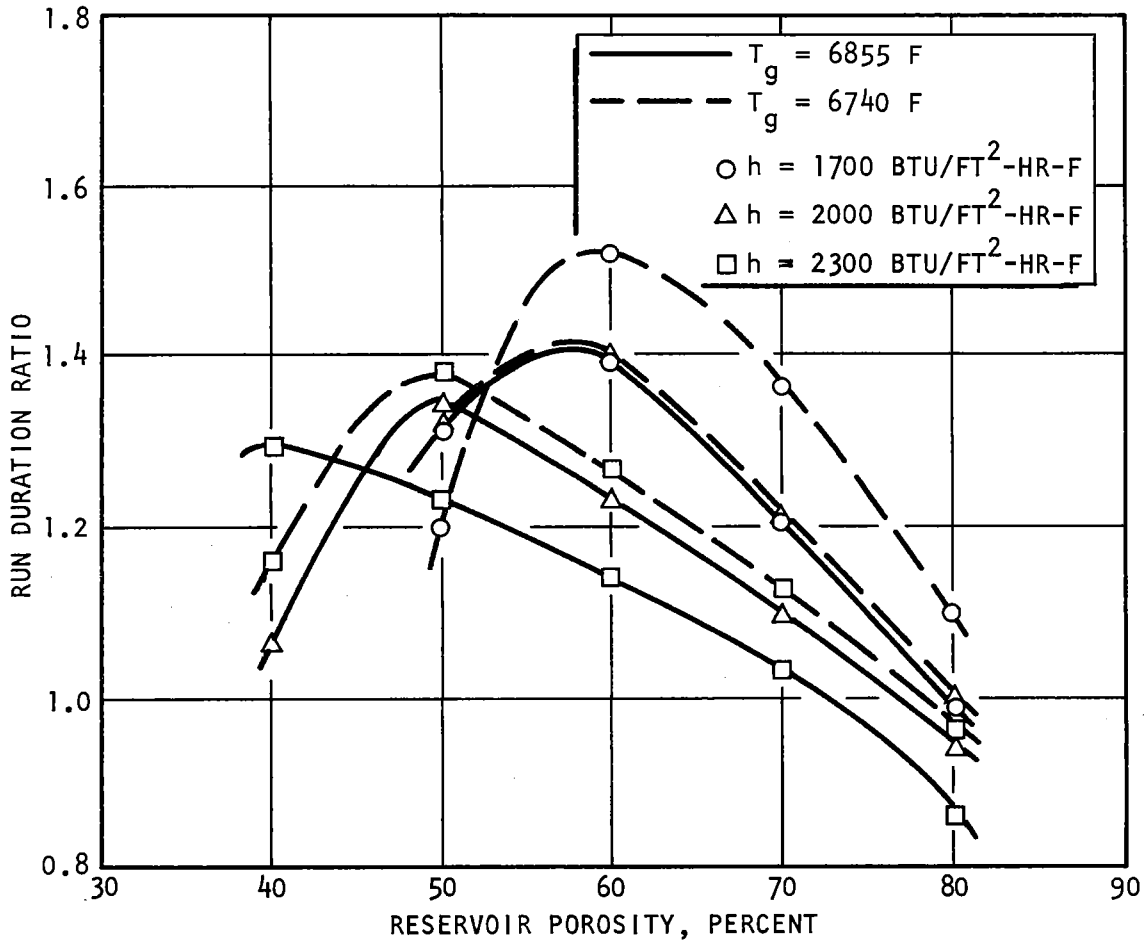

Figure 6. Comparison of Run Duration with Self-Cooled and Dense Tungsten Throat Inserts Under Identical Nozzle Throat Conditions (Predicted)

(combining convection and radiation) increase, surface melting becomes the failure mode, and lower porosity, high-conductivity matrices are preferable. Conversely, for less severe thermal conditions, coolant depletion limits insert lifetime and more porous matrices must be used. With the exception of the least severe thermal conditions studied, a maximum improvement of 30 to 40 percent over a dense tungsten heat sink was calculated for reservoir porosities of 40 to 60 percent. For the least severe case, the calculated lifetime improvement was slightly over 50 percent.

The effect of varying the high-density throat layer thickness is shown in Fig. 7. Cases analyzed considered inserts of 60 percent reservoir porosity exposed to h = 2000 Btu/ft^2-hr-F for gas temperatures of 6855 and 6740 F. From Fig. 6, the optimum structure at the lower gas temperature contained the 1/8-inch thick throat layer. Increasing throat layer thickness sharply reduced the calculated lifetime as coolant depletion, due to reduced overall matrix porosity, became limiting. At the higher gas temperature, the 1/8-inch thick throat layer with 60 percent reservoir porosity was not optimum. Increasing throat layer thickness would provide only a slight improvement in life expectancy by increasing insert thermal conductivity. However, as in the preceding case, early failure would occur by depletion if throat layer thickness were increased beyond 1/4-inch. The latter case also indicated that reservoir porosity was the controlling parameter, since, from Fig. 6, it was shown that an insert with a 1/8-inch thick throat layer and 50 percent reservoir porosity would have a significantly increased lifetime over a 60 percent porous design under the same thermal conditions.

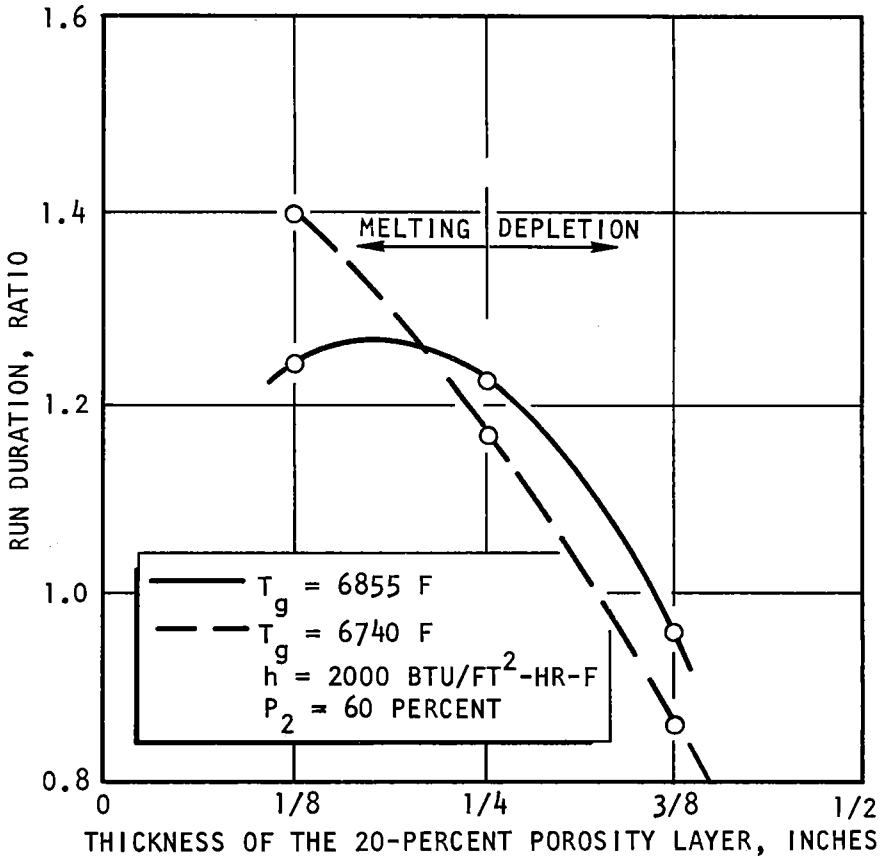

Figure 7. Effect of the Low-Porosity Throat Layer Thickness on Insert Lifetime

SELF-COOLED NOZZLE APPLICATION

Application Range

The results of the design analysis can be used to identify a range of practical application of self-cooling rocket nozzle throat inserts. From the preceding, the relative performance of a self-cooled insert can be best compared with a counterpart heat sink. The most significant increases in potential service lifetimes of self-cooled composites over a tungsten heat sink occur in applications in which the flame temperature is only slightly above the tungsten matrix melting point. Since surface temperature tends to approach the melting point asymptotically in this case, failure will occur by coolant depletion. Furthermore, optimization becomes critical since lifetime is very sensitive to changes in matrix porosity. This point is demonstrated by data in Table 7, results of computations performed on a zinc-cooled duplex-porosity composite exposed to 6200 F gas with h = 2000 Btu/ft^2-hr-F (Ref. 3). A similar trend illustrating the criticality of optimization for the less severe thermal conditions was shown in Fig. 6, in which the curves tend to peak more as gas temperature and heat transfer coefficient decrease.

TABLE 7

LIFETIMES OF ZINC-INFILTRATED COMPOSITES OF VARIOUS RESERVOIR POROSITIES FOR Tg = 6200 F AND h = 2000 Btu/ft^2-hr-F (Ref. 3)

Reservoir Porosity, percent	Service Lifetime, seconds	Duration Ratio Relative to a Tungsten Heat Sink
20	19	0.30
80	84	1.31
90	184	2.88

As gas temperature increases, failure by surface melting becomes limiting, and less porous matrix designs become necessary. Consequently, total lifetime increases of self-cooled inserts become less compared to a dense tungsten heat sink. For the thermally most severe of the cases in the present study, a maximum improvement of approximately 30 percent could be attained by an optimum self-cooled composite over a heat sink; however, the increase represented only an 8-second longer potential lifetime (exclusive of the heat sink capacity of the coolant-depleted matrix). Therefore, nozzle heat flux and gas temperature conditions approaching those of the most severe case studied probably represent a practical application limit. Achievement of longer insert lifetimes for flame temperatures approaching 7000 F at heat transfer coefficients in excess of 2000 Btu/ft^2-hr-F would require supplemental thermal protection.

Extended Applications

The inherent simplicity and reliability of self-cooling thermal protection make the concept especially attractive for solid-fuelded rocket nozzles. However, as described in the preceding section, lifetime capability of self-cooled inserts, while still superior to heat sinks, may not be sufficient for the extreme thermal conditions expected in advanced high-performance motors. Alternative active thermal protection techniques, such as convection or transpiration cooling, have the capability for long duration firings; but, inherent performance losses and the requirements for additional propellants, pressurization and fluid transport hardware, metering and controls are decided disadvantages. Extension of self-cooled composite application for long duration service under more severe thermal conditions would be preferable. The design analysis indicated several techniques are possible to extend the self-cooling thermal protection concept.

Since matrix melting was shown to necessitate lifetime-limited low-porosity structures for very high gas temperatures, substitution for tungsten by a more refractory matrix material is an obvious remedy. Porous graphite might be considered as an insert liner. However, lack of adequate corrosion resistance to aluminized propellant exhaust gas species weighs against graphite application. Application of extremely refractory carbides or similar high-melting compounds is another possibility. Reduced thermal conductivity relative to tungsten must be considered, but the use of such a material may be confined to the throat layer. In fact a porous overlay structure of very high melting point and low thermal conductivity on the nozzle throat surface can act as a thermal barrier to a tungsten substrate and acts to reduce net heat transfer to the insert. Furthermore, problems of structural integrity and thermal shock sensitivity common with carbides are lessened if these materials are applied as a relatively thin overlay to a structural matrix.

Another approach to increase potential insert lifetime in a relatively low porosity matrix is to use a coolant with a greater volumetric latent heat of vaporization than zinc but with similar vapor pressure characteristics. All the simple, elemental coolants have been evaluated based on thermophysical properties, metallurgical and chemical compatibility, and fabricability and zinc appeared optimum for high throat gas pressure applications (Ref. 2). Alternatively, alloys or compounds may be able to combine properties not attainable by a single element. For example, brass might combine the high volumetric heat of vaporization of copper with the high vapor pressure of zinc (Ref. 9, 23). Similarly, compounds of high heat of formation may dissociate into species of low molecular weight to provide an additional blocking effect at the throat wall (Ref. 2). The low thermal conductivity of compounds is a disadvantage for self-cooled composites.

Reduction of the film heat transfer coefficient by vapor blocking may also be accomplished by injection of low molecular weight gas species up-stream of the nozzle throat. For example, combination of a low temperature "gas generator" grain may be used to form a protective layer (Ref. 24). Similarly, ablative sections placed up-stream of the nozzle can provide a similar effect. The resultant reduction in heat transfer coupled with an optimized self-cooled insert design could combine to give adequate service lifetime without resort to more complex active thermal protection schemes.

EXPERIMENTAL INSERT DESIGN

Design Objectives

To satisfy program objectives, two experimental insert designs were to be tested by NASA-LRC. Design A was to have had longer lifetime, achieved through optimized matrix porosity. Two inserts of Design A were to be fired under identical conditions to establish design consistency. Design B, to be fired under the same conditions as Design A, was to have had a shorter life expectancy through reduced matrix porosity and coolant storage capacity.

Design calculations for model insert exposed to the anticipated throat conditions of the NASA-LRC 18-inch hybrid motor indicated that a reservoir porosity of 50 percent would be optimum. For a structure with a 1/8-inch thick throat layer, nozzle lifetime was predicted to be 30 to 40 percent greater than for a tungsten heat sink. Comparison with prior NASA-LRC hybrid motor firings (Table 6) indicated an expected minimum service lifetime for Design A of between 39 to 42 seconds, depending on actual flame temperature and heat transfer coefficient.

Reduction in expected service lifetime for Design B was accomplished by reducing matrix reservoir porosity to 40 percent. Reference to Figure 4 indicated a 15 to 30 percent improvement over a heat sink with a 40 percent

porous structure backing a 1/8-inch thick throat layer. Comparison with previous test firing data (Table 6) suggested an expected 32 to 33 second lifetime.

Confidence in analytical predictions must be tempered by several additional considerations. The analysis considered a two-dimensional infinite annulus geometry where the most severe heat ransfer conditions were imposed over the entire surface. In contrast, the real nozzle insert has a convergent throat geometry with different heat fluxes imposed over the throat surface, and heat transfer is not necessarily radial. A significant complication would be non-uniform recession of coolant within the matrix, a factor which would affect temperature distribution and coolant utilization. Predictions of service lifetime were made on the basis of surface melting or coolant exhaustion. In the former case, actual insert failure, as evidenced by erosion-induced chamber pressure decay, may occur before the surface reaches the melting point because of material weakness at temperatures approaching 6100 F. In the case of predicted failures due to coolant depletion, the heat capacity of the matrix may be sufficient to extend service lifetime for a few additional seconds by heat sink cooling. The latter effect may be especially important for low-porosity matrix structures.

Insert Configuration

Experimental inserts were of the sintered four-step construction developed under a previous program (Ref. 3). The inserts consisted of a two-piece throat surface layer, the up-stream surface being relatively impermeable with respect to the downstream surface, a high-porosity coolant reservoir section, and an outer low-permeability, high-density encapsulating layer. The structural elements of the insert are shown in Fig. 8.

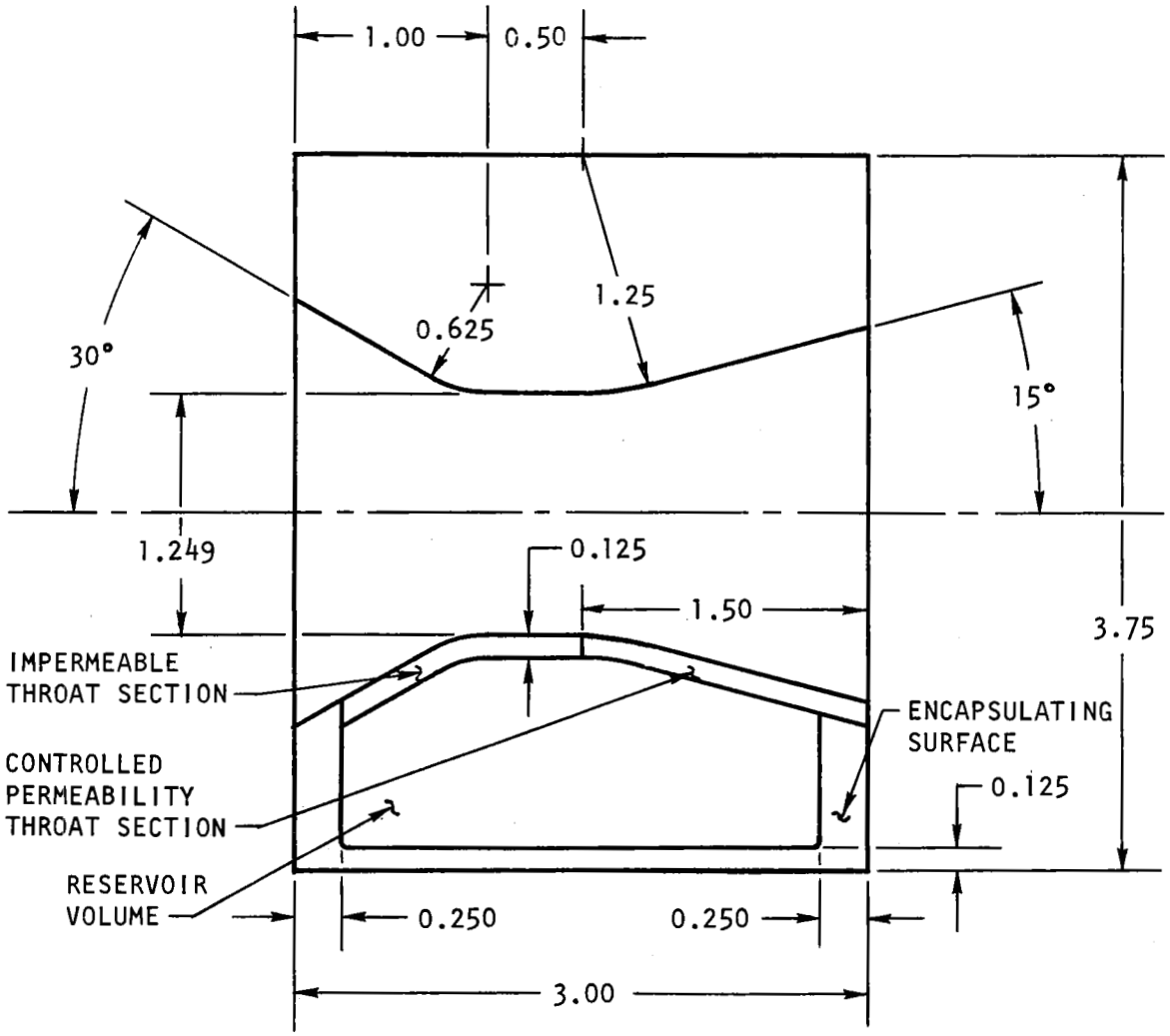

Figure 8. Design A Self-Cooled Nozzle Insert

The function of the graded permeability throat surface layer is to prevent entry of high-pressure exhaust gas species into the up-stream portion of the insert. Furthermore, the two-piece design permits venting of coolant vapor into a region of low throat pressure. The permeability of the downstream throat surface section controls internal coolant vaporization temperature and flowrate.

Insert Designs A and B were to be identical in all respects with the exception of the porosity of the reservoir. Design A, to have the longer service lifetime capability, had a reservoir porosity of 50 percent; and, Design B, 40 percent.

Nozzle Assembly

The self-cooled nozzle inserts were retained in an assembly compatible with the standard nozzle housing used on the NASA-LRC 18-inch hybrid motor to provide for direct installation. A schematic of the nozzle assembly for the self-cooled inserts is presented in Fig. 9. The steel case and locking ring were furnished by NASA-LRC, and the throat contour was identical to NASA-LRC design drawings (Ref. 25).

The self-cooled insert was surrounded by a cylindrical graphite heat sink insulated from the balance of the retainer assembly by a layer of zirconia. This design minimizes heat conduction from the insert into the surrounding hardware and simulates the limited heat sink capacity of volume-restricted flight-weight nozzle designs.

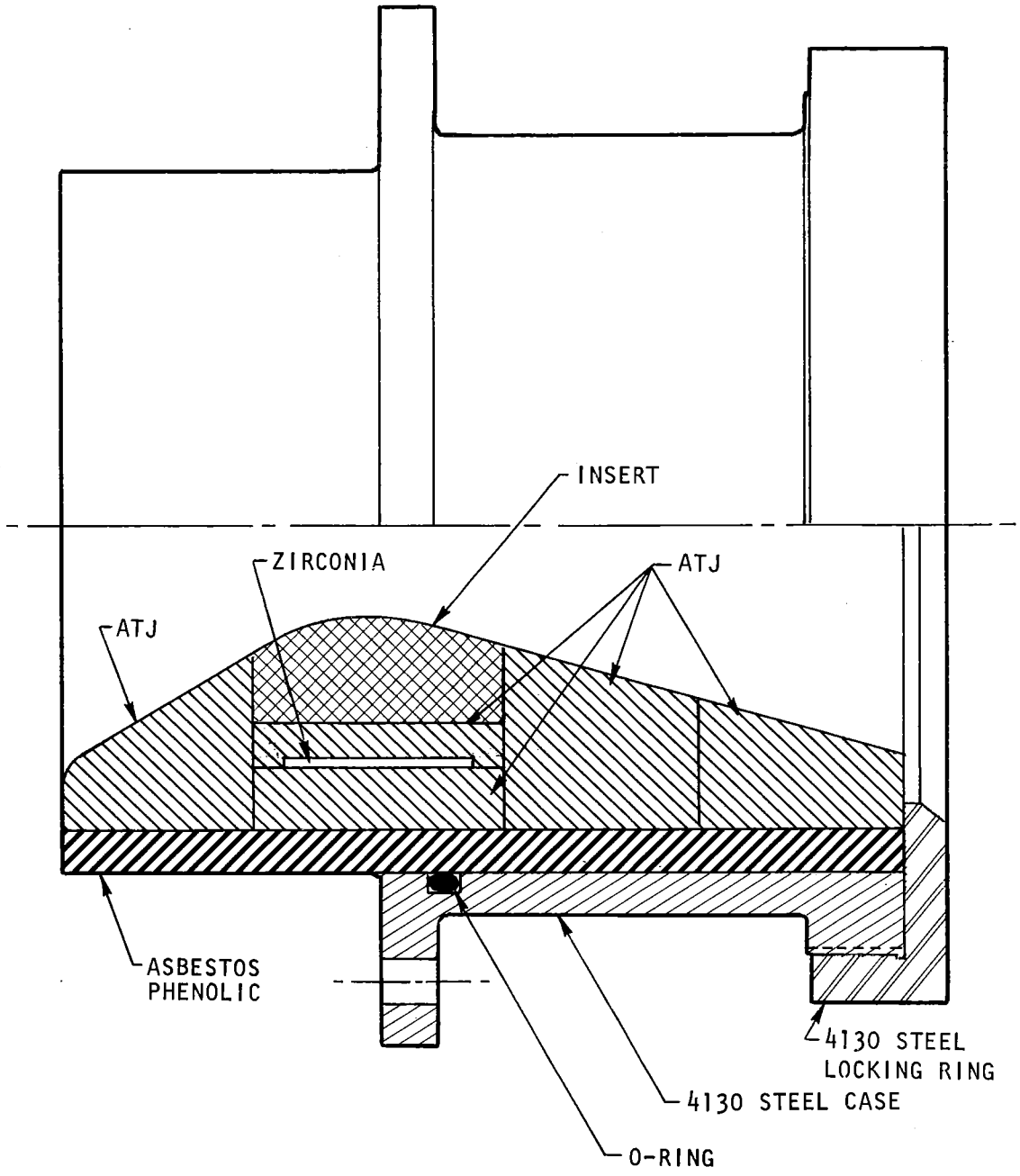

Figure 9. Nozzle Assembly for NASA-LRC Hybrid Motor

SELF-COOLED INSERT FABRICATION

POWDER METALLURGY APPROACH

The sequential cold isostatic compaction process was used to fabricate graded-porosity test inserts. Individual elements of porous structure were compacted sequentially to build up the desired insert configuration.

In a body containing various types of widely differing porosities, individual powder compositions must be tailored not only to produce the requisite final microstructure but also to ensure compaction and sintering compatibility. For example, during sequential consolidation, compaction of subsequent elements must not distort or rupture a previously compacted element. The reverse may also happen in that cracking in an as-pressed layer may occur as a result of elastic relaxation of an under layer during pressure release.

Many difficulties can be avoided by maximizing compact green strength. Within limits imposed by final microstructural requirements, green strength may be improved by powder compositional changes such as finer particle size, use of irregular particles, or the addition of a binder.

If compositional changes alone cannot produce the necessary green strength improvement, modifications may also be made to molding and compacting procedures. Compaction pressures may be adjusted to yield maximum strength with least relaxation of compacted volumes. In the case of sequential isostatic pressings of concentric structures, it was found that compaction pressures should be reduced as the outer layers were pressed (Fig. 1). This procedure minimized the elastic deformation of underlying layers and the subsequent relaxing spring-back that may lead to rupture of the just-pressed outer layers. The inner layers may be compacted at a sufficiently high pressure to permit

required compaction pressure reductions for subsequent layers. Finally, green strength improvements may be accomplished by changes in mold geometry to reduce compact stresses as by a simple increase in as-pressed section thickness to reduce residual tensile stress. Excess material may then be subsequently removed by machining after compaction or sintering. Similarly, the elimination of stress concentrations, such as at sharp corners, mitigates the requirements for compact green strength.

Unequal densification of various powder mixtures during sintering may lead to distortion or fracture of a graded porosity compact. For example, those fine powders of high specific surface area used to form low-permeability units characteristically mold and compact to low relative densities, but they subsequently sinter to high densities, producing large volumetric shrinkage. Conversely, coarse powders of low specific surface area (e.g., spherically shaped) readily compact but may not densify appreciably during sintering. To minimize unequal sintering shrinkage within a graded porosity body, binary powder mixtures (i.e., blends of closely-sized coarse and fine powders) were used (Ref. 3). Binary mixtures, in which the coarse particle diameter is several times larger than the fine, pack to greater densities and exhibit less sintering shrinkage. In addition, the porous properties of sintered mixtures in which the volume of fines exceeds 20 percent closely resemble those of matrices consisting of pure fines. It is, therefore, possible to match sintering shrinkages with the appropriate binary mixtures of similar microstructure.

Sintering shrinkage may also be controlled by the magnitude of the compaction pressure and by the times and temperatures of presintering and sintering treatments. In general, high compaction pressures and prolonged low-temperature presintering decrease the sintering density change of single-sized powder, powder with pore-former additions, or binary mixtures. The sintering treatments must also ensure microstructural stability so that the porous body will not densify further in elevated temperature service. Thus, a final sinter may also act as a presinter with respect to the anticipated operating temperature.

DESIGN A INSERT

The Design A insert was fabricated according to the plan shown in Fig. 8 with reservoir porosity of 50 percent. The upstream throat surface was to be impermeable relative to the downstream section. An encapsulating layer of minimum porosity and permeability was to act as structural support and coolant seal.

Spherical tungsten powder* was used in the controlled permeability, downstream throat section. Spherical powder characteristically forms thermally stable structures of predictable porous properties. Spherical powder was also added for shrinkage control to fine irregular powder** to form the impermeable, upstream throat section and the encapsulating layer. Ammonium carbonate, added as pore-former, and the fine irregular tungsten powder was the mixture used to form the high-porosity reservoir layer. Powder compositions for the various insert layers are presented in Table 8. Stearic acid dissolved in acetone was added as a binder.

TABLE 8

DESIGN A INSERT TUNGSTEN POWDER MIXTURE COMPOSITIONS

Structural Element	Powder Composition
Upstream Throat Section, Encapsulating Layer	82% "G" Tungsten, 6.85-micron F.S.S.S. 14.5% -200 +325 mesh Spherical Tungsten 2.0% -200 mesh Ammonium Carbonate 1.5% Stearic Acid (in acetone)
Controlled Permeability, Downstream Throat Section	99.5% -325 mesh Spherical Tungsten 0.5% Stearic Acid (in acetone)
Reservoir Section	91.2% "G" Tungsten 8.8% -200 mesh Ammonium Carbonate

* Supplied by Federal-Mogul, Warren, Michigan, 99.9-percent pure.

**Firth-Sterling, Type G High-Purity Tungsten Powder

Sequential isostatic compaction was used to build up the graded structural matrix. The throat layer was pressed around a contoured stainless steel mandrel sized to compensate for sintering shrinkage. The mandrel could be mounted in a lathe to machine the as-pressed layers to final contour. Molds for isostatic compaction were fabricated by dipping patterns in uncured polyvinyl chloride (PVC). The mold for pressing the throat layer was contoured in a shape corresponding to the mandrel profile. Molds for the reservoir and outer layer were simple cylindrical bags. The nozzle compaction sequence and respective compaction pressures were as follows:

1. Throat layer, upstream and downstream sections pressed simultaneously at 45,000 psig.
2. Reservoir section at 30,000 psig.
3. Encapsulating layer at 10,000 psig.

The sintering process involved outgassing, pre- and final-sintering cycles. A portion of the volatile ammonium carbonate pore-former was removed prior to heating by vacuum outgassing overnight in the sintering furnace. Subsequently, the furnace was back-filled with hydrogen to 1/3-atmosphere pressure, and the compact heated slowly (1 F/min.) for 4 hours to remove the remainder of the ammonium carbonate pore-former and stearic acid binder. The heating rate was then increased to 6 F/min. to 2330 F for a 2-hour presinter which was followed by evacuating the furnace and heating to 3030 F for an additional 2-hour vacuum presinter. Final sintering was accomplished under vacuum for 4 hours at 4000 F. After sintering, the insert was infiltrated with zinc under hydrogen atmosphere at 1250 F for 15 minutes.

DESIGN B INSERTS

The Design B self-cooled nozzle insert was modified with respect to Design A as follows (Fig. 10):

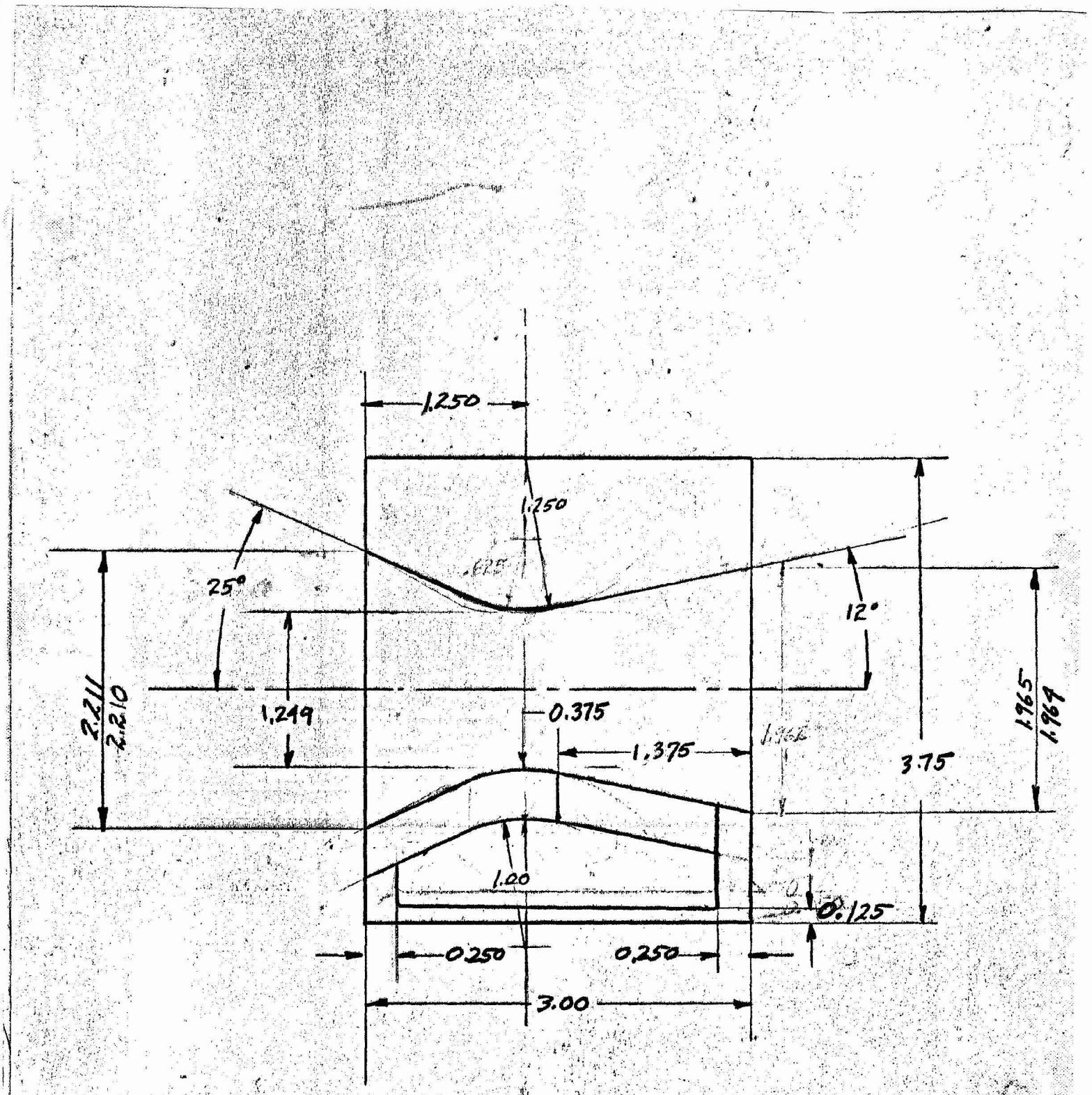

Figure 10. Design B Self-Cooled Nozzle Insert.

1. The throat layer thickness was increased to 0.375 inches (from 0.125 inches).

2. The interface between up-and-downstream throat sections was moved aft 0.125 inches.

3. The throat contour had a continuous contour to a minimum throat diameter in contrast to the flat throat of Design A.

4. Entrance and exit angles were slightly changed to fit the nozzle assembly (Fig. 9).

The compositions of the upstream throat and encapsulating layers for the Design B inserts are presented in Table 9. Shortage of spherical powder of the same type as that used in the first insert required modification in powder composition for the second insert. Pressing and sintering procedures were the same for both Design B inserts and were identical to those reported above for Design A.

TABLE 9

DESIGN B UPSTREAM THROAT SECTION AND ENCAPSULATING LAYER POWDER COMPOSITIONS

	Weight Percent	
Powder	Insert 1	Insert 2
"G" Tungsten	82	78.5
-200 +325 mesh Spherical Tungsten	14.5	18.0
-200 mesh Ammonium Carbonate	2.0	2.0
Stearic Acid (in acetone)	1.5	1.5

All other portions of the Design B type nozzles, encapsulating layer, controlled permeability downstream throat section, and reservoir section were in accordance with Table 8 in regard to composition.

FIRING PROGRAM

NASA-LRC HYBRID GAS GENERATOR

The motor used for self-cooled insert testing is a 1500-lb. thrust, 18-inch diameter hybrid propellant gas generator (Ref. 25) utilizing a solid binder + 45-percent aluminum fuel and nitrogen tetroxide oxidizer. The binder consisted of a polyurethane formulation: 38.75%BDR-15, 2.63% 2,4-TDI, 11.62% Tufflo Oil, 2% Elftex 5. Ignition is achieved by injection of Aerozine 50 into the combustion chamber for approximately three seconds at the start of firing. A 300 psig nitrogen purge was provided at test termination to extinguish the grain and protect the insert from excessive post-test oxidation.

DESIGN A TEST

Pretest inspection of the Design A self-cooled nozzle insert revealed an area of surface roughness in the exit portion corresponding to the spherical powder throat section. The roughness was located in the lower half of the insert, as mounted in the test motor, at approximately 6 o'clock. Surfaces mating graphite and the nozzle insert were smooth with no gaps. The insert was not potted into the graphite with any adhesive.

Actual test parameters for the Design A test are presented in Table 10. A 24.5-pound fuel residue remained after firing. Chemical analysis of the residue indicated that it consisted of 55.1 weight percent metallic aluminum and 5.5 weight percent acid-insoluble non-combustibles.

The chamber pressure trace for the test firing is presented in Fig. 11. Apparent throat erosion, causing a rapid chamber pressure drop, occurred 11 seconds after ignition. After an action time of 33 seconds, chamber pressure had dropped 50 percent to 400 psig, and the test was terminated by valving off oxidizer flow and initiating the nitrogen purge.

1. The throat layer thickness was increased to 0.375 inches (from 0.125 inches).

2. The interface between up-and-downstream throat sections was moved aft 0.125 inches.

3. The throat contour had a continuous contour to a minimum throat diameter in contrast to the flat throat of Design A.

4. Entrance and exit angles were slightly changed to fit the nozzle assembly (Fig. 9).

The compositions of the upstream throat and encapsulating layers for the Design B inserts are presented in Table 9. Shortage of spherical powder of the same type as that used in the first insert required modification in powder composition for the second insert. Pressing and sintering procedures were the same for both Design B inserts and were identical to those reported above for Design A.

TABLE 9

DESIGN B UPSTREAM THROAT SECTION AND ENCAPSULATING LAYER POWDER COMPOSITIONS

	Weight Percent	
Powder	Insert 1	Insert 2
"G" Tungsten	82	78.5
-200 +325 mesh Spherical Tungsten	14.5	18.0
-200 mesh Ammonium Carbonate	2.0	2.0
Stearic Acid (in acetone)	1.5	1.5

All other portions of the Design B type nozzles, encapsulating layer, controlled permeability downstream throat section, and reservoir section were in accordance with Table 8 in regard to composition.

FIRING PROGRAM

NASA-LRC HYBRID GAS GENERATOR

The motor used for self-cooled insert testing is a 1500-lb. thrust, 18-inch diameter hybrid propellant gas generator (Ref. 25) utilizing a solid binder + 45-percent aluminum fuel and nitrogen tetroxide oxidizer. The binder consisted of a polyurethane formulation: 38.75%BDR-15, 2.63% 2,4-TDI, 11.62% Tufflo Oil, 2% Elftex 5. Ignition is achieved by injection of Aerozine 50 into the combustion chamber for approximately three seconds at the start of firing. A 300 psig nitrogen purge was provided at test termination to extinguish the grain and protect the insert from excessive post-test oxidation.

DESIGN A TEST

Pretest inspection of the Design A self-cooled nozzle insert revealed an area of surface roughness in the exit portion corresponding to the spherical powder throat section. The roughness was located in the lower half of the insert, as mounted in the test motor, at approximately 6 o'clock. Surfaces mating graphite and the nozzle insert were smooth with no gaps. The insert was not potted into the graphite with any adhesive.

Actual test parameters for the Design A test are presented in Table 10. A 24.5-pound fuel residue remained after firing. Chemical analysis of the residue indicated that it consisted of 55.1 weight percent metallic aluminum and 5.5 weight percent acid-insoluble non-combustibles.

The chamber pressure trace for the test firing is presented in Fig. 11. Apparent throat erosion, causing a rapid chamber pressure drop, occurred 11 seconds after ignition. After an action time of 33 seconds, chamber pressure had dropped 50 percent to 400 psig, and the test was terminated by valving off oxidizer flow and initiating the nitrogen purge.

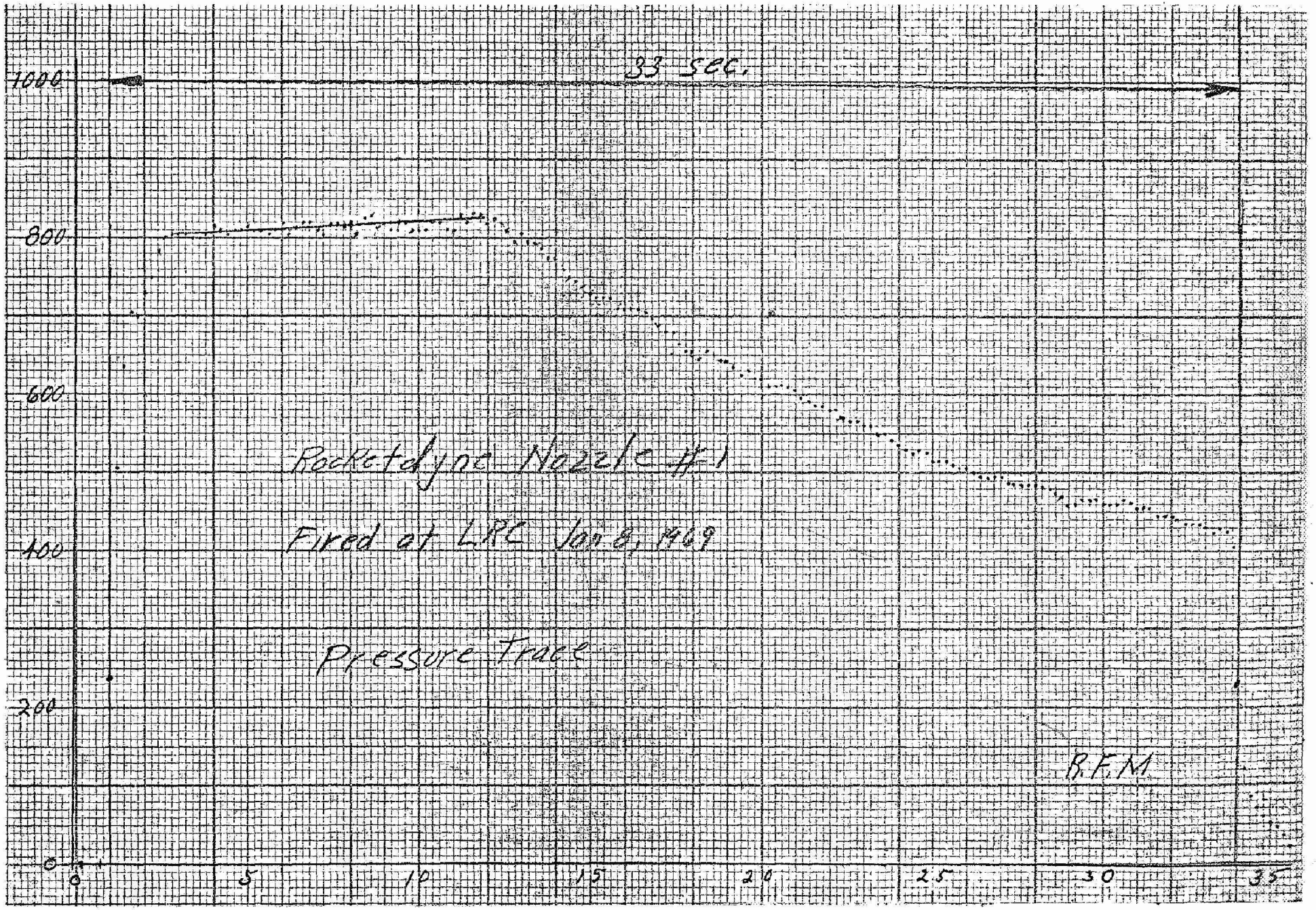

Figure 11. Design A Test Firing
Chamber Pressure Trace

TABLE 10

DESIGN A INSERT TEST PARAMETERS

Parameter	Value
Firing Time, sec.	33
Fuel Consumption, lb./sec.	1.98
Oxidizer Flowrate, lb./sec.	4.67
Mass Flow, lb./sec.	6.65
O/F Ratio	2.36
Chamber Pressure, psig	800
Chamber Temperature, F	6800
Throat Diameter, in.	1.249

Post-test inspection of the nozzle assembly revealed severe damage of the insert (Fig. 12,13). The majority of damage to the insert appeared as a slot in the 6 o'clock position.

Closer inspection of the insert after nozzle disassembly showed complete loss of the throat surface with the reservoir section substantially eroded out (Fig. 14) and a deep groove cut in the aft insert surface (Fig. 15). Disassembly also revealed considerable fuel residue in the lower portion of the motor chamber (Fig. 16).

Figure 12. Entrance Side of As-Fired Design A Nozzle Assembly.

Nozzle from entrance side after test
of 1-8-68

Below [TOP] slightly off heater
and that dry slot was close to bar

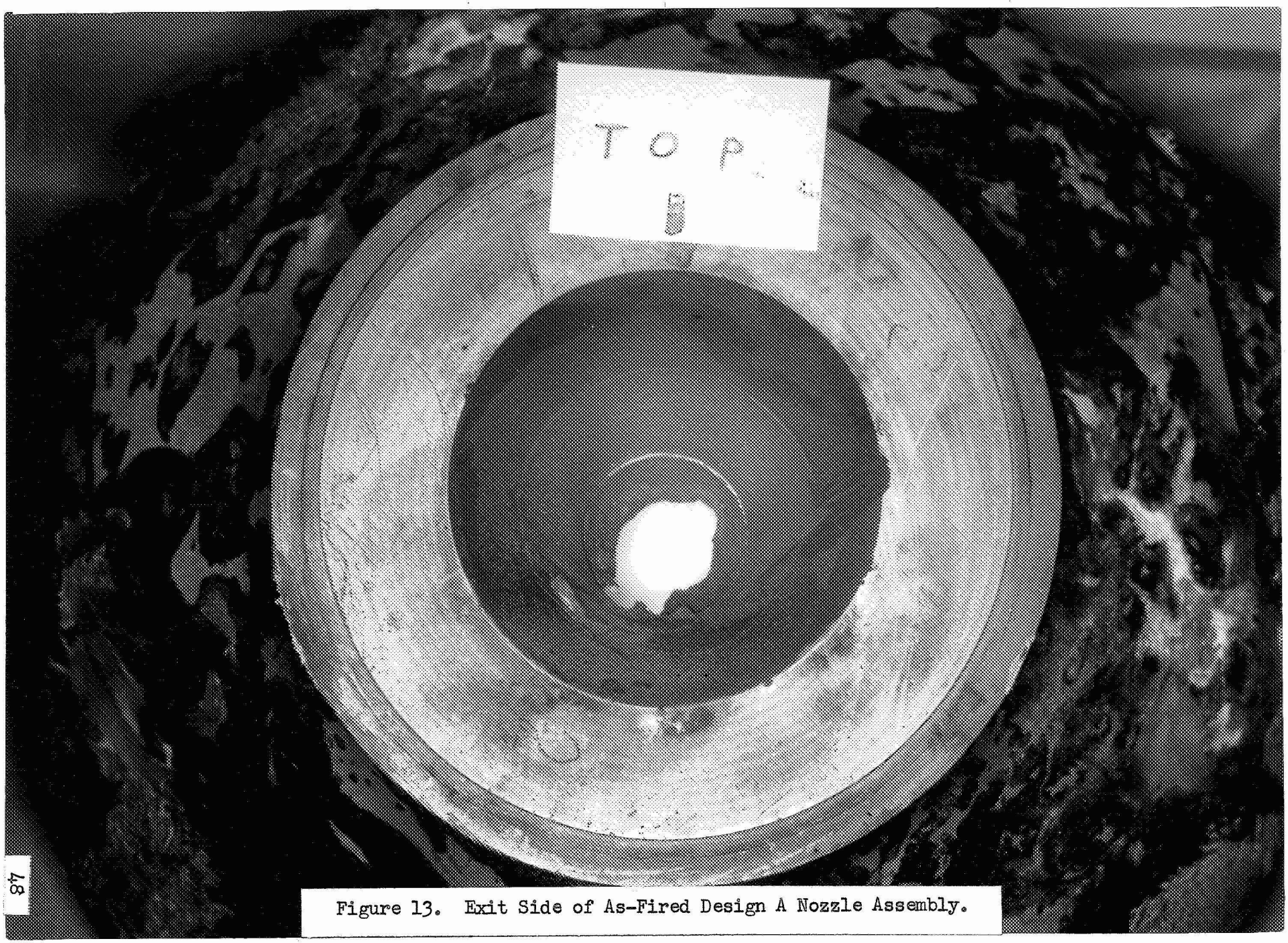

Figure 13. Exit Side of As-Fired Design A Nozzle Assembly.

Noe a [illegible] test of 1-8-69

Accuracy of 70P [illegible]

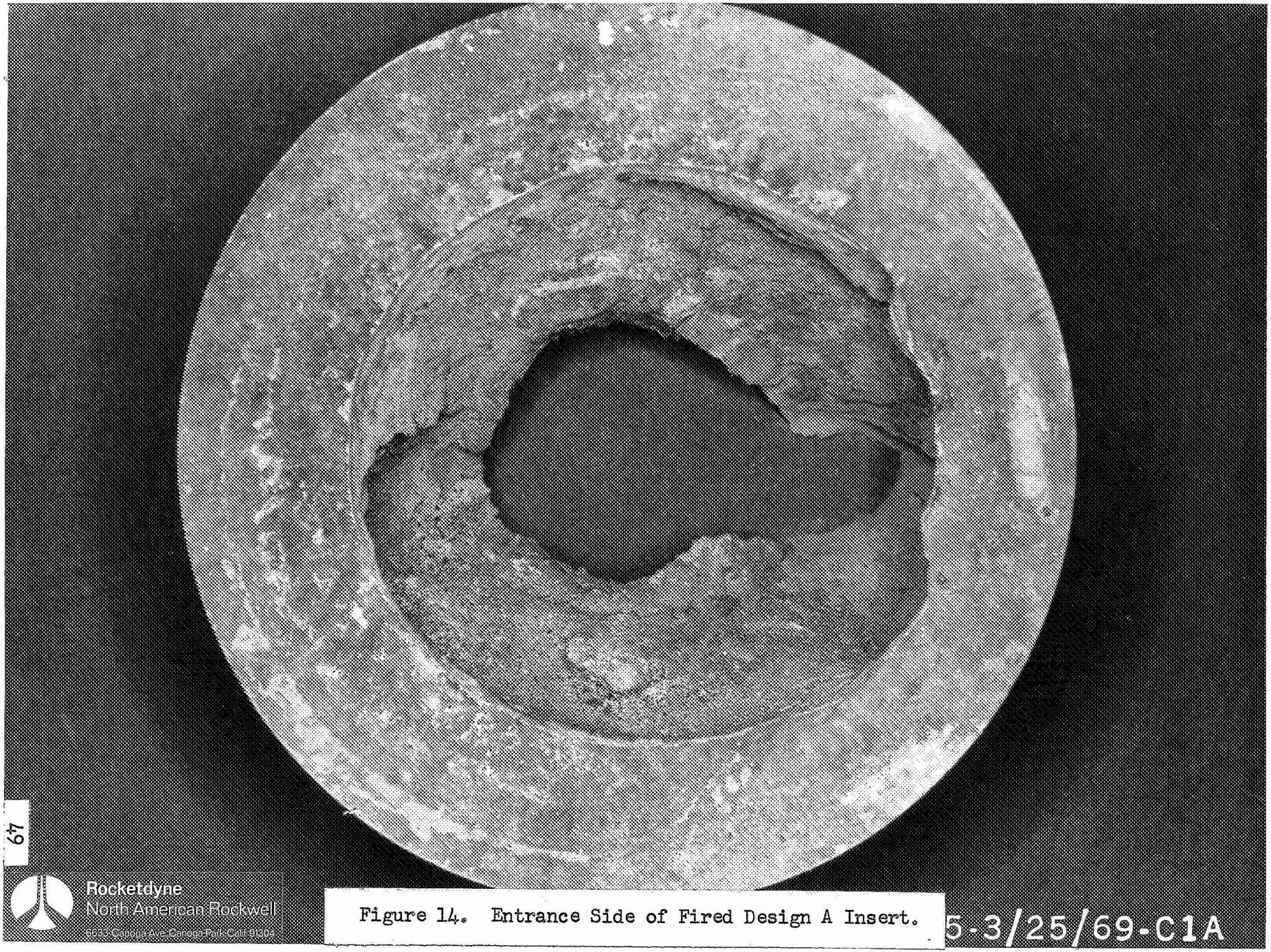

Figure 14. Entrance Side of Fired Design A Insert.

5-3/25/69-C1A

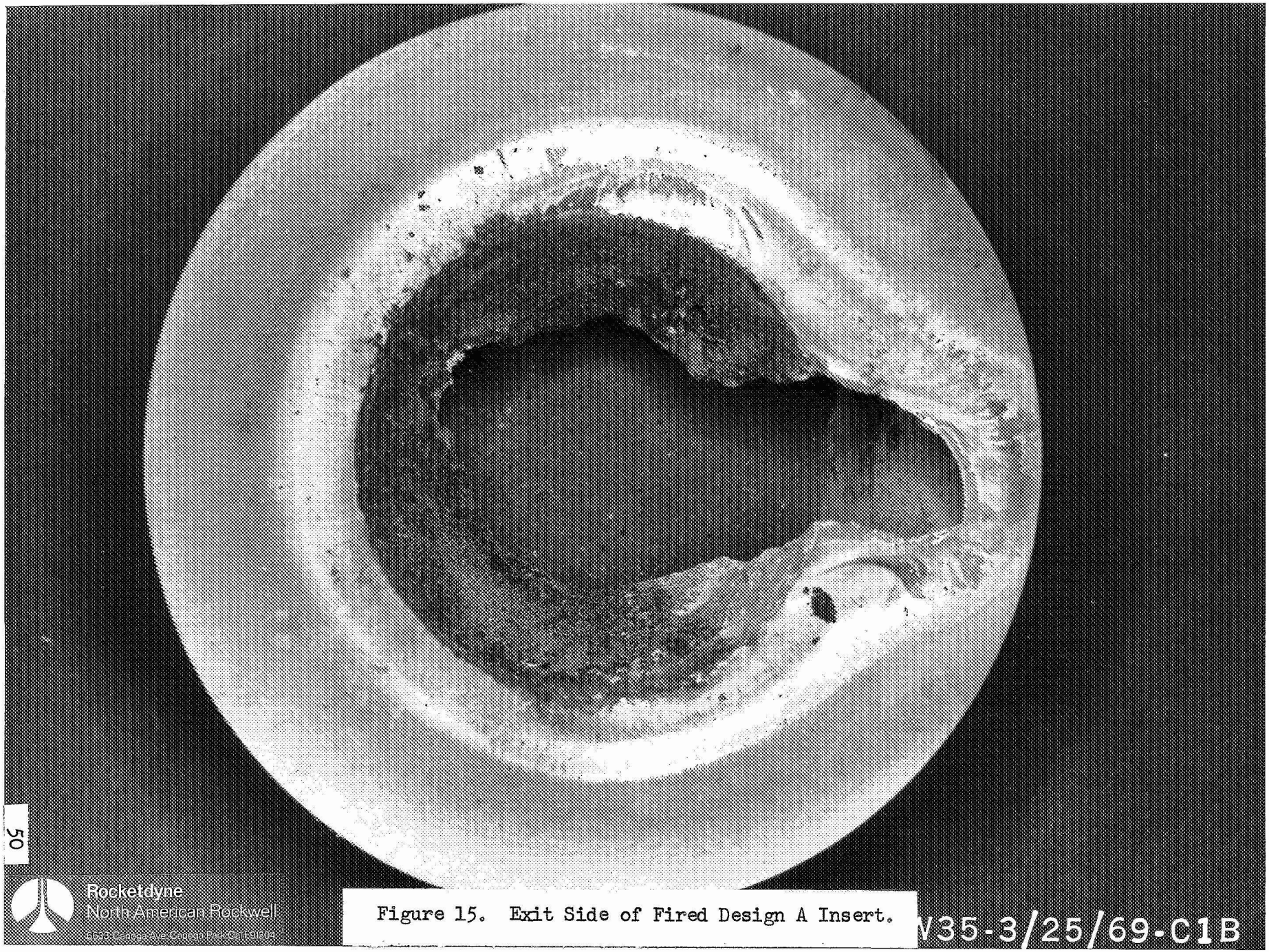

Figure 15. Exit Side of Fired Design A Insert.

V35-3/25/69-C1B

Figure 16. Fuel Residue Remaining in Aft End of Mixer After Design A Firing.

Aft End of [illegible] after test of 1-[illegible]

1-9-[illegible]

DISCUSSION OF DESIGN A TEST RESULTS

The loss of chamber pressure after a 12-second action time fell considerably short of the anticipated 39-42 seconds predicted by the computer analysis. Several factors, singly or combined, may have contributed to premature insert erosion:

1. A nozzle insert defect, possibly that noted in the pretest examination at the exit end, and corresponding to the deep grooving formed in the graphite retainer
2. More severe thermal conditions (e.g., heat transfer coefficient or flame temperature) than originally anticipated
3. Direct attack of the insert throat by uncombusted, free liquid aluminum

The latter may be a distinct possibility since it is suspected by NASA-LRC personnel that at most one-third of the aluminum loading in the grain is burned. Similarly, in NASA-LRC tests with a lithium-loaded grain in a hybrid system, uncombusted liquid lithium has been known to puddle and subsequently burn through a graphite nozzle leaving a groove in the lower half as observed in the present test. Furthermore, liquid aluminum is extremely aggressive with respect to intergranular attack of tungsten. Such a condition could only be aggravated under the high-temperature, high-pressure conditions of the test and the porosity of the insert.

If test conditions were more severe than anticipated, the 50-percent porous reservoir section of the insert would not have been optimum. For example, with a heat transfer coefficient of 2300 Btu/ft^2-hr.-F and a flame temperature of 6855 F, failure may have been predicted to occur within 31 seconds instead of 39 to 42 seconds predicted for a somewhat

lower heat transfer coefficient or flame temperature. However, even this time is longer than the failure time experienced, and the actual mechanism of nozzle erosion may have been a combination of factors involving throat environment and insert properties. For example, failure times predicted by the analysis are based on either the occurrence of surface melting or coolant depletion. However, it is possible that erosion could occur prior to the time that the throat surface reaches the matrix melting temperature. In fact, intergranular attack by aluminum could so severely weaken the insert throat section that erosion could occur well below the melting point.

Whether or not a nozzle insert defect was present cannot be determined since all the evidence was essentially destroyed. Post-fabrication inspection indicated complete infiltration of the matrix with the zinc coolant. With the exception of the indication of roughness in the exit as noted above, no other potential defects were found. Extreme care was taken in the machining of the insert so as to assure proper thickness of the throat layer. Nonetheless, the possible presence of a defect must be considered since positive proof to the contrary is unobtainable.

In view of the possibility of highly erosive conditions at the throat entrance, the insert was redesigned with a thicker throat layer. Thus, Design B had a 0.375-inch throat layer thickness compared to 0.125 inch for Design A. The increased throat layer thickness also would reduce total insert porosity, thereby increasing matrix thermal conductivity to reduce throat surface temperature.

CONCLUSIONS

Calculations performed under the present program with the modified Self-Cooled Nozzle Computer Program substantiated the criticality of microstructure on performance under a given set of nozzle throat service conditions. A trade-off in matrix porosity, balancing coolant storage capacity and insert thermal conductivity, was the most important optimization parameter.

Application of self-cooled inserts is limited by a combination of flame temperature and heat transfer coefficient which requires that the optimum composite for the given thermal conditions has too low a matrix porosity (viz., high insert thermal conductivity) for adequate coolant storage and, therefore, lifetime potential.

Premature failure due to throat erosion during the test firing of the Design A insert was probably due to motor operating conditions, such as a fuel-rich combustion condition, not anticipated in the theoretical nozzle performance analysis. The Design A insert was inadequate in terms of throat layer thickness for the motor conditions realized in the test. The Design B insert would compensate for the motor conditions, through a thicker throat layer and reduced overall matrix porosity.

The original program objectives were not achieved due to the curtailed test firing program.

Unanticipated additional funds were expended in refabricating inserts found defective on final inspection. In one case, the defect was associated with an error in machining. In a second case, extensive cracking of the outer layer had occurred during sintering. Additional funds were unavailable. Although problems due to the peculiarities of the test motor were critical, they would not have been sufficient to stop the program prior to completion since the Design B insert took those peculiarities into account.

RECOMMENDATIONS

1. Extend the Self-Cooled Nozzle Computer Program to a three-dimensional model.
2. Test fire the two Design B inserts in a motor with more predictable performance than the NASA-LRC 18-inch hybrid.

REFERENCES

1. Gessner, F. B. et al, "Summary Report, Self-Cooled Rocket Nozzles," Volume 2, RTD-TDR-63-4046 (U), Air Force Materials Laboratory, Research and Technology Division, AFSC, Wright-Patterson Air Force Base, Ohio, March 1964.

2. Schwarzkopf, P. and E. D. Weisert, "Summary Report, Self-Cooled Rocket Nozzles," Volume 1, RTD-TDR-63-4046 (C), Air Force Materials Laboratory, Research and Technology Division, AFSC, Wright-Patterson Air Force Base, Ohio, March 1964, CONFIDENTIAL.

3. Schwarzkopf, P. and E.D. Weisert, "Self-Cooled Rocket Nozzles," Volume 3, RTD-TDR-63-4046, Air Force Materials Laboratory, Research and Technology Division, AFSC, Wright-Patterson Air Force Base, Ohio, August 1965.

4. Cronin, L.J., material presented at the Second Shock Tube Symposium, Air Force Special Weapons Center, Palo Alto, California, 6 March 1958.

5. O'Conner, T. and T. Smith, "Ablation Test Results for Infiltrated Tungstens" (Task 4.2 - High Performance Tip Materials - REST Program), RAD-TM-64-31, AVCO Corporation, Wilmington, Massachusetts, 21 July 1964, CONFIDENTIAL.

6. Panel on Thermal Protection, NASA Research Advisory Committee on Materials, "Thermal Protection Systems," NASA Technical Memorandum X-650, Washington, D.C., February 1962, CONFIDENTIAL.

7. Smith, W.E. and G.F. Davies, "Development of Refractory Materials for Rocket Nozzles and Vanes," Summary Report, Clevite Corporation, Cleveland, Ohio, Contract NOrd 18887, 19 May 1960.

8. Baranow, S. and R.H. Hiltz, "The Performance and Application of Infiltrated Tungsten Structures as Inserts in Solid Propellant Rocket Nozzles," ARS-2413-62, American Rocket Society, April 1962.

9. Robinson, A.T.R., et al, "Nozzle Development for Hybrid Propulsion System," NAVWEPS, Report 7802, NOTS TP 2798, U.S. Naval Ordnance Test Station, China Lake, California, 14 November 1961, CONFIDENTIAL.

10. "Microtranspiration, A Protective Mechanism for Rocket Nozzle Throat Materials," The Bendix Corporation, South Bend, Indiana, 1 June 1961.

11. "Development of Tungsten - Beryllia Oxide Rocket Nozzles," National Beryllia Corporation, Haskell, N.J., Contract NOrd 18039, 31 May 1960.

12. Owen, L., Jr. and E. Cliffel, Jr., "Development of Refractory Materials for Rocket Nozzles and Vanes," Summary Report, Clevite Corporation, Cleveland, Ohio, Contract NOrd 18887, 7 June 1964.

13. Resnick, R., et al, "Cooling of Porous Tungsten Structures by Evaporation of Infiltrated Material," Metals Eng. Quarterly 3 (2) 51 (1963).

14. Perez, M., "Optimum Utilization of Impregnated Throat Inserts in Rocket Nozzles by Surface Encapsulation and Preferential Venting," Preprint No. 64-105, Solid Propellant Rocket Conference, Palo Alto, California, January 29-31, 1964.

15. Levy, A. V., "Composite Materials for Solid Rocket Nozzles," Bulletin of the Interagency Solid Propellant Rocket Meeting, Vol. III; p. 397, July 1963.

16. "Investigation of Solid State Transpiration Cooling of Rocket Engine Thrust Chambers and Nozzles and Fabrication of Hardware," Summary Report No. HTC-62-7, Hughes Tool Company, Culver City, California, Contract AF04(611)-6075, January 1962, CONFIDENTIAL.

17. "A Feasibility Demonstration of a Thermo-Structural Nozzle for Solid Propellant Rocket Motors," Technical Report No. 65-179, AF Rocket Propulsion Laboratory, AFSC, Edwards AFB, California, August 1965, CONFIDENTIAL.

18. Shewmon, D. C., "Development of High-Temperature Materials for Rocket Nozzles and Associated Structures," Summary Report, Clevite Corporation, Cleveland, Ohio, Contract NOw 64-0232-C, 30 November 1965.

19. Sturiale, T., et al, "Development of Manufacturing Methods for the Production of Infiltrated Tungsten Composite Nozzle Inserts," AFML-TR-66-316, Air Force Materials Laboratory, AFSC, Wright-Patterson AFB, Ohio, December 1966.

20. Price, J., "Design, Fabrication and Evaluation of Tungsten Encapsulated Silver Infiltrated Porous Tungsten Rocket Nozzle Inserts," NASA CR-66759, ARDE-Portland, Inc., Paramus, New Jersey, Contract NAS 1-4722.

21. Gerhauser, J. N. and R. J. Thompson, Jr., "Theoretical Performance Evaluation of Rocket Propellants," R-5802, Rocketdyne, A Division of North American Rockwell Corporation, Canoga Park, California, 3 August 1964.

22. Bartz, D. R., "A Simple Equation for Rapid Estimation of Rocket Nozzle Convective Heat Transfer Coefficients," Jet Propulsion, 27, 49 (1957).

23. White, J. E. and D. H. Leeds, "A Metallurgical Evaluation of Various Infiltrated Tungsten Materials in Arc and Nitrogen Plasmas," J. Spacecraft, 3 (7) 1051 (1966).

24. Sutton, G. P., et al, "Advanced Cooling Techniques for Rocket Engines," Astronautics and Aeronautics, 4 (1) 60 (1966).

25. HTM-18 Motor Assembly, Drawing No. 7300-208 Rev. A, United Technology Center, Sunnyvale, California.